Title

Strawberry phenotypic plasticity in flowering time is driven by interaction between genetic loci and temperature

Alexandre Prohaska[a,b], Aurélie Petit[b], Silke Lesemann[c], Pol Rey-Serra[a], Luca Mazzoni[d], Agnieszka Masny[e], José F. Sánchez-Sevilla[fg], Aline Potier[a], Amèlia Gaston[a], Krzysztof Klamkowski[e], Christophe Rothan[a], Bruno Mezzetti[d], Iraida Amaya[fg], Klaus Olbricht[c], Béatrice Denoyes[a]

[a]Univ. Bordeaux, INRAE, Biologie du Fruit et Pathologie, UMR 1332, F-33140, France
[b]INVENIO, MIN de Brienne, 110 quai de Paludate, 33800 Bordeaux, France
[c]Hansabred GmbH & Co. KG, Dresden, Germany
[d]Department of Agricultural, Food and Environmental Sciences, Marche Polytechnic University, 60131 Ancona, Italy
[e]National Institute of Horticultural Research, Konstytucji 3 Maja 1/3, 96-100 Skierniewice
[f]Centro IFAPA de Málaga, Instituto Andaluz de Investigación y Formación Agraria y Pesquera (IFAPA), 29140, Málaga, Spain
[g]Unidad Asociada de I+D+i IFAPA-CSIC Biotecnología y Mejora en Fresa, 29010, Málaga, Spain.

alexandre.prohaska@inrae.fr, a.petit@invenio-fl.fr, Silke.Lesemann@gmx.de, pol.rey-serra@inrae.fr, l.mazzoni@staff.univpm.it, agnieszka.masny@inhort.pl, josef.sanchez@juntadeandalucia.es, aline.potier@inrae.fr, amelia.gaston@inrae.fr, krzysztof.klamkowski@inhort.pl, christophe.rothan@inrae.fr, b.mezzetti@staff.univpm.it, iraida.amaya@juntadeandalucia.es, k.olbricht@hansabred.org, beatrice.denoyes@inrae.fr

Date of submission: 29/11/2023
Number of tables and figures: 3 and 5 respectively
Word count (excluding materials and methods): 5219
Supplementary data: Number of tables and figures: 13 and 5 respectively

ORCID A. Prohaska: https://orcid.org/0009-0004-0395-7470

ORCID A. Petit https://orcid.org/0000-0003-1577-9072

ORCID P. Rey-Serra https://orcid.org/0000-0002-3685-2470

ORCID L. Mazzoni https://orcid.org/0000-0001-6749-4621

ORCID A. Masny https://orcid.org/0000-0002-6727-5653

ORCID Jose Sanchez-Sevilla https://orcid.org/0000-0002-6690-7196

ORCID A. Gaston https://orcid.org/0000-0001-9974-8083

ORCID K. Klamkowski https://orcid.org/0000-0003-0358-3726

ORCID C. Rothan: https://orcid.org/0000-0002-6831-2823

ORCID B. Mezzetti https://orcid.org/0000-0001-9307-812X

ORCID I. Amaya https://orcid.org/0000-0002-4612-8902

ORCID K.Olbricht https://orcid.org/0000-0003-1124-2585

ORCID B. Denoyes: https://orcid.org/0000-0002-0369-9609

* Corresponding author:

Béatrice Denoyes

Phone number: +33 (0)5 57 12 24 60

Email: beatrice.denoyes@inrae.fr

Highlights

A GXE study of a segregating strawberry population in Europe showed that temperature is the main driver of flowering time plasticity. A genetic marker was designed for the main QTL.

Running title

Strawberry phenotypic plasticity in flowering time

Abstract

The flowering time, which determines when the fruits or seeds can be harvested, is known to be sensitive to plasticity, i.e. the ability of a genotype to display different phenotypes in response to environmental variations. In the context of climate change, strawberry breeding can take advantage of phenotypic plasticity to create high-performing varieties adapted either to local conditions or to a wide range of climates. To decipher how the environment affects the genetic architecture of flowering time in cultivated strawberry (*Fragaria ×ananassa*) and modify its QTL effects, we used a bi-parental segregating population grown for two years at widely divergent latitudes (5 European

countries) and combined climatic variables with genomic data (Affymetrix® SNP array). We detected 10 unique flowering time QTL and demonstrated that temperature modulates the effect of plasticity-related QTL. We propose candidate genes for the three main plasticity QTL, including *FaTFL1* which is the most relevant candidate in the interval of the major temperature-sensitive QTL (6D_M). We further designed and validated a genetic marker for the 6D_M QTL which offers great potential for breeding programs, for example for selecting of early-flowering strawberry varieties well adapted to different environmental conditions.

Key words: flowering time, genotype × environment interaction (G×E), phenotypic plasticity, QTL-by-Environment Interaction (QEI), Quantitative Trait Locus (QTL), strawberry

Introduction

Phenotypic plasticity describes the ability of a given genotype to produce distinct phenotypes in response to different environments (Pigliucci, 2005). It allows species, populations, or genotypes to cope with rapid environmental changes, including global climate change. In crop species, knowledge of trait plasticity is an important element of the success of a variety. The breeder can select locally adapted varieties which, by taking advantage of local conditions, will give better results than widely adapted varieties (Ceccarelli, 1989; Kusmec et al., 2018).

The central approach to characterize plasticity of a trait is to identify for each genotype the reaction norm, which describes how the target phenotype of a specific genotype varies as a function of the environmental variables to which the genotype is exposed (Sultan, 1987). Genotype-by-environment interactions (G×E) are observed when reaction norms are non-parallel between genotypes (Pigliucci, 2005). To assess this interaction, multiple genotypes or populations must be studied in a large range of environments. Numerous statistical approaches have been developed to study this interaction (reviewed in Li et al., 2017). G×E can be detected by an ANOVA with fixed or mixed models but the interpretation of the interaction is limited with these approaches. Other approaches such as AMMI or joint regression model allow the estimation of plasticity parameters to explain the interaction. Factorial regression allows the inclusion of explicit environmental factors (i.e. covariates) in G×E models along with a direct evaluation (i.e. quantification) of the importance of these covariates for G×E explanation (Malosetti et al., 2013; Lombardi et al., 2022). As a consequence, this model makes it possible to identify the environmental parameters that are biologically relevant to the trait.

One of the traits described as highly sensitive to plasticity is flowering time (Blackman, 2017). It is a trait critical for the adaptation of a variety to a particular region, as it determines when fruits or seeds are harvested and the final yield. It is regulated by endogenous genetic components and environmental factors (Cho et al., 2017). Strawberry (*Fragaria ×ananassa*), the most cultivated berry worldwide with a total harvested area of 389,665 ha and a total production of 9,175,384 T in 2021 (FAOSTAT, https://www.fao.org/faostat/en/#data), is widely grown in the northern and southern hemispheres. New varieties adapted to a wide range of latitudes, from tropical/subtropical to cold temperate climates, have been selected using different strategies (Senger et al., 2022). Varieties cover more or less restricted regions: for example, 'Fortuna' is grown in Florida (USA) but also in Mexico, Spain, Egypt and Morocco and, conversely, 'Florence' is restricted to Norway. As most breeding programs are organized according to seasonality, the genetic architecture of flowering time and its plastic responses to environments need to be characterized (Li et al., 2018). Unlike perpetual flowering (PF) mutants where flowers are initiated continuously, flowering in seasonal flowering (SF) genotypes occurs in spring and is the consequence of floral initiation that occurred the previous autumn under low temperature and short days (Gaston et al., 2020, 2021). Thus, after dormancy, plant growth resumes in spring and inflorescences initiated the previous year emerge and flower. While the genetic and molecular control of floral initiation has been extensively studied in diploid species (Iwata et al., 2012; Koskela et al., 2012; Gaston et al., 2020 and 2021) and, more recently, in cultivated octoploid strawberry (Nakano et al., 2015; Koembuoy et al., 2020; Gaston et al., 2021; Muñoz-Avila et al., 2022), studies on the genetic control of flowering time are scarce and focus exclusively on diploid species (Samad et al., 2017).

Exploring how flowering time and its phenotypic plasticity are genetically and environmentally controlled is essential for breeding better adapted strawberry varieties. To achieve this objective, we built a concerted European project (GoodBerry) to study the response of flowering time to diverse environments in a bi-parental segregating population cultivated at very different latitudes (5 southern and northern European countries) over a two-year period. The integration of strawberry genomic data (Affymetrix® SNP array) with phenotypic and climatic data enabled us to detect three flowering time quantitative trait loci (QTL) for which the overall mean flowering times co-localized with plasticity parameters. We further designed and validated a genetic marker for the main highly temperature-sensitive QTL (6D_M), which offers strong potential for selecting strawberry varieties well adapted to different climates.

Material and methods

135

136 **Plant material and phenotyping**

137 A pseudo full-sibling F1 population of 109 individuals derived from two SF varieties with contrasting
138 European cultivation areas was obtained: 'Candonga' is widely cultivated in south of Spain and
139 'Senga Sengana', originally selected in Germany, is commonly grown in Poland. Nine experiments
140 were conducted in five countries from north and south Europe in 2018 (5 experiments) and 2019 (4
141 experiments): Skierniewice, Poland (PL) (51°95´N); Dresden, Germany (GE) (51°05´N); Agugliano, Italy
142 (IT) (43°32N); Douville, France (FR) (45°59´N); and Huelva, Spain (SP) (37°24´N) (Fig. 1A). To
143 homogenise the physiological development of daughter plants of all individuals and parents, young
144 plants obtained from a single nursery were sent to the five locations for plantation in 2017 and 2018
145 (Supplementary Fig. S1). For each individual of the genetic segregating population, 10 plants were
146 grown in open field or under plastic tunnels, except in France where they were grown in soil-free
147 pine bark substrate under plastic tunnel. Flowering time was defined as the date of observation of
148 the first flower at anthesis.

149

150 At each location, we recorded daily climatic variables, temperatures (mean, maximum, minimum; in
151 °C) and global radiations (in kw/m²). These data were analysed by hierarchical clustering using
152 Euclidean distance and Ward's method. The distance was calculated based on environmental
153 parameters: temperatures (mean, maximum, minimum, difference minimum-maximum per day),
154 photoperiod, global radiation and sum of Growing Degree-Days (GDD) of the nine environments.

155

156 **Modeling flowering time**

157 To model flowering time phenology, we tested four thermal time models: Growing Degree-Days
158 (GDD, Wang, 1960), triangular (Hänninen, 1990a), sigmoid (Hänninen, 1990b) and Wang (Wang and
159 Engel, 1998). These models assume that there is a relationship between the phenological stage (the
160 flowering period) and the cumulative temperature above a threshold (base temperature, Tb or Tmin)
161 over a given period. Temperature is expressed here in degrees Celsius (Chuine et al., 1998). This sum
162 (SStar) is calculated from the starting date, t0. In addition, triangular and Wang models consider
163 optimal (Topt) and maximal (Tmax) temperatures. In addition, to study the efficiency of predicting
164 flowering date as a function of photoperiod or global radiation, we adapted the calculation of the
165 GDD and triangular models to these two climatic parameters. Process-based models were adjusted
166 by minimizing the residual sum of squares with the simulated annealing algorithm of Metropolis
167 (Chuine et al., 1998) using the Phenology Modeling Platform software (PMP5;
168 http://www.cefe.cnrs.fr/fr/recherche/ef/forecast/phenology-modelling-platform) (Chuine et al.,
169 2013). Adjustment was repeated 20 times to ensure that the global optimum had been reached. To

simulate the flowering time, we included data from both parents and from 102 individuals for whom all the data for the nine environmental conditions were available. For further analyses, we retained the most parsimonious model and the best efficiency (R^2).

Statistical modeling for variance components and heritability estimation

To study the variation in flowering time (GDD) in our segregating population, we fitted a linear mixed-effects model (LMM) by maximum-likelihood (LME4 package; Bates et al., 2015) following equation 1 (eqn1):

$$Y_{ijk} = \mu + \underline{G_i} + E_j + \underline{(G \text{ x } E)_{ij}} + \varepsilon_{ijk}$$

where μ is the overall mean of the population, Gi the random effect of genotype i, Ej the fixed effect of environment i, G x Eij the random interaction effect between genotype i and environment j and eijk the residual term assumed to be normally distributed. The best sub-model was selected according to Fisher test for the environment effect log-likelihood ratio tests (LRT) for random effects with the lmerTest R package (Bates et al., 2021). The selected model was re-fitted by Restricted Maximum Likelihood with the plantTrialLmmFitCompSel function from the rutilstimflutre R package (Timothee Flutre's personal R code. URL https://github.com/timflutre/rutilstimflutre).

The broad-sense heritability at the whole design level (H2) was derived from the variance components of eqn1 and calculated in equation 2 (eqn2):

$$H^2 = \frac{{\sigma^2}_G}{\left({\sigma^2}_G + \frac{{\sigma^2}_{G\times E}}{n_{environment}} + \frac{{\sigma^2}_\varepsilon}{n_{rep.environment} \times n_{environment}}\right)}$$

with genotype (G) variance (σ^2) at the numerator. Random variance components involving environment (E) were divided by the number of environments ($n_{environments}$). Residual variance was divided by the number of environments multiplied by the average number of replicates per environment ($n_{rep.environment}$).

Statistical modeling of plasticity parameters

We performed complementary statistical approaches to compute genotype specific plasticity parameters using the additive main effects and multiplicative interaction (AMMI) method, the joint regression analysis also named Finlay-Wilkinson (FW) regression model and the factorial regression model.

(i) The additive main effects and multiplicative interaction (AMMI) method combines analysis of variance (ANOVA) to model main effects of genotype and environment and principal component analysis (PCA) to decompose the complex structure of G×E into Interactive Principal Component Axes (IPCA) (Gauch, 2013) (equation 3, eqn3):

$$Y_{ij} = \mu + G_i + E_j + \sum_{k=1}^{K} (\lambda_k \alpha_{ik} \gamma_{jk}) + \varepsilon_{ij}$$

where Y_{ij} is the mean phenotypic performance of genotype i in environment j; μ is the intercept; G_i the fixed effect of genotype i; e_j is the fixed effect of environment j; λ_k is the singular value for the IPCA k; α_{ik} are the genotypic IPCA scores and γ_{jk} the environmental loadings for axis k; ε_{ij} is the residual term G×E not captured by the model and some error deviation.

We derived AMMI Stability Value (ASV) from eqn3 for each genotype as the relative influence of IPCA1 and IPCA2 scores based on their interaction sum of squares (SS) according to Purchase (1997) using the formula:

$$ASV = \sqrt{\left[\left(\frac{SS_{IPCA1}}{SS_{IPCA2}}\right) \times IPCA1\right]^2 + IPCA2^2}$$

where (SS_{IPCA1}/SS_{IPCA2}) is the weight assigned to the IPCA1 value by dividing the IPCA1 SS by the IPCA2 SS; IPCA1 and IPCA2 scores were the genotypic scores derived from the AMMI model. A large positive ASV value indicates a genotype that is adapted to particular environments. A small (close to zero) ASV value indicates a stable genotype across environments (Bakare et al., 2022).

(ii) In the joint regression analysis (FW regression), G×E is modeled by regressing mean phenotypic performance of genotypes on an environmental index. The index value of each environment is calculated as the mean of all individuals of the flowering time in that environment (Finlay and Wilkinson, 1963). Then, the intercept and slope for each genotype are calculated by regressing genotypic performance on the environmental index as in equation 4 (eqn4):

$$Yij = \mu + G_i + (1 + \beta_i) \times E_j + \varepsilon_{ij}$$

where $\mu+G_i$ represents the average performance of a genotype considering all environments; the slope $1+\beta_i$ represents the regression coefficient of the model and is the linear response to environment; the residual variance of the term ε, which measures the scatter of points about the regression lines, represents the non-linear response to environment (non-linear plasticity).

(iii) The factorial regression model allowed the description of G×E by using explicit covariates as environmental factors (Tmean, Tmin, Tmax, GDD, photoperiod or global radiation). Each climatic covariate was tested successively at a significance threshold of 5% to be incorporated into the following equation 5 (eqn5):

$$Yij = \mu + G_i + E_j + \alpha_i \times Cv_j + \varepsilon_{ij}$$

where the genotypic response of genotype i in environment j is described through its sensitivity α_i to the tested covariate Cv_j. Slopes from eqn4 and eqn5 were computed with the script adapted from Diouf et al. (2020).

Other statistical analyses

Correlations between the mean flowering times were performed with "rcorr" procedure of the Hmisc R package (https://cran.r-project.org/web/packages/Hmisc/Hmisc.pdf) and a Bonferroni correction was applied at a threshold of 5%. Pairwise comparisons were performed using Student's T-test ($p < 0.05$).

Development of linkage maps

Single dose markers (SD) from the Affymetrix® array (Hardigan et al., 2020) that were in backcross configuration and segregated 1:1 (Rousseau-Gueutin et al., 2008) were used for genetic map construction using JoinMap® 5.1 software (Van Ooijen, 2011). Grouping was performed using independence log of the odds (LOD) and the default settings in JoinMap®. Linkage groups (LG) were chosen from a LOD higher than 10 for all of them. Map construction was performed using the maximum likelihood (ML) mapping algorithm and the parameters described in Labadie et al. (2022). Mapping results are displayed using MapChart (Voorrips, 2002).

QTL mapping and QTL-by-environment interactions (QEI)

The female and male linkage parental maps based on the 109 individuals were used separately for QTL analysis. Flowering time expressed as GDD by environment and plasticity parameters (i.e. ASV and IPCA values from AMMI model, slopes and residual variances from joint and factorial regressions), represented the phenotypic data. QTL detection was performed by simple interval mapping (SIM) using R/QTL package (Broman et al., 2003). Permutation analysis (1000 permutations) was performed to calculate the critical LOD score. QTL with LOD values higher than the LOD threshold at $p \leq 0.05$ were considered significant. When one QTL was found significant, we used composite interval mapping (CIM) with one co-variable at the position of the significant QTL and reiterated the analysis until no new significant QTL were detected. Bayesian credible interval was

calculated using the function 'bayesint' at probability of 0.95. The proportion of phenotypic variance explained by a single QTL was calculated as the square of the partial correlation coefficient (R^2).

We searched for QTL × temperature by SIM following a two-step procedure by testing the temperature as an interactive (eqn6)

$$Yij = \mu + \beta_t . t_j + \beta_g . g_i + \gamma . t_j . g_i + \varepsilon_{ij}$$

and then as an additive (eqn7) covariate:

$$Yij = \mu + \beta_t . t_j + \beta_g . g_i + \varepsilon_{ij}$$

where Yij is the trait value for allele i (i = 1,2) in environment j among the nine location-by-year combinations (overall mean of the flowering time); t_j, the mean temperature in environment j; g_i, the QTL effect for genotype i; γ, the QTL × temperature interaction coefficient; ε_{ij}, the residual term. Evidence of QEI was assessed by taking the LOD difference between equations 6 (eqn6) and 7 (eqn7).

Candidate genes

Candidate genes likely to play a role in flowering time were identified into the Bayesian credible intervals common to the different QTL detected in each region showing the highest number of significant QTL: 3A_M, 6A_M and 6D_M. Homologs of known flowering time genes were selected as candidate genes in 'Camarosa' (Edger et al., 2019) and 'Royal Royce' (Hardigan et al., 2021; https://phytozome-next.jgi.doe.gov/info/FxananassaRoyalRoyce_v1_0) genomes.

Marker design

We developed a subgenome-specific Kompetitive Allele Specific PCR (KASP) marker (Smith and Maughan, 2015) linked to the major 6D_M QTL. The Affymetrix® marker AX-184201950 localized in the middle of the QTL harbours a C/T SNP (Hardigan et al., 2020). Specific primer design was performed using BatchPrimer3 software (http://probes.pw.usda. gov/batchprimer). Genotyping was done on the segregating population and on additional 94 genotypes using the KASP procedures described by LGC Genomics (Supplementary Table S1). Genotyping data were viewed as a cluster plot (LightCycler® 480 qPCR software, Roche). The significance of the relationship between phenotype and genotype was determined using Wilcoxon test.

Results

Strawberry flowering time plasticity under natural conditions

We studied the flowering time of the 'Candonga' x 'Senga Sengana' strawberry bi-parental population cultivated in five countries covering a wide range of latitudes (Fig. 1A; Supplementary Table S2). Cultures were conducted under field (PL, GE, IT) or tunnel (FR, SP) environments. Flowering time was measured during two successive years 2018 and 2019 (hereafter named 18 and 19), except Spain, which was only measured in 2019, and thus nine location-by-year combinations. These nine environments clustered into two groups that overlapped southern (SP, IT, FR) and northern (GE, PL) areas in Europe (Fig. 1B).

The bi-parental population was issued from a cross between two varieties displaying geographical opposite cultural adaptation with 'Candonga' selected in Southern Europe and 'Senga Sengana' in Northern-Eastern Europe (Fig. 1C). Flowering time followed a latitude gradient when expressed as calendar days and showed a larger variation in southern environments than in northern ones (Fig. 1D). At Northern latitudes, the population flowered on average six to eight days earlier in 2018 than in 2019 (Fig. 1D). Notably, phenotypic correlations between environments were strictly positive but were weak (0.27-0.59) (Fig. 1E; Supplementary Table S3) suggesting genotype-by-environment interactions with changes in ranking.

Growing Degree Days (GDD) for expressing the flowering time

In strawberry, temperature has been described as the main environmental factor affecting the flowering time (Le Mière et al., 1998; Opstad et al., 2011) whereas photoperiod has been reported to influence flowering time in PF genotypes (Sønsteby and Heide, 2007) or global radiation in SF genotypes (Krüger et al., 2022). We tested four models: GDD, triangular, sigmoid and Wang based on temperatures, global radiation and/or photoperiod. Whatever the model, the best efficiency was obtained with thermal times and Tmean (85%) (Table 1). Models were not improved by adding the effect of global radiation or photoperiod. Estimates of the parameters for each model were also similar for both the base temperature (Tb), -1.7—1.8 °C except for the Wang model (-13.6 °C), and the starting date (t0), January 1st. The triangular and Wang models gave in addition an optimum temperature (Topt) at 24-25 °C and a maximum temperature (Tmax) at 34-35 °C. This temperature was not reached under our conditions and we therefore retained the most parsimonious GDD model for further analysis.

We hypothesized that genotypes differed in the heat units necessary to trigger flowering. Therefore, we calculated the GDD value of each individual with parameters t0 as the 1st of January and Tb as -

1.7°C. We further plotted reaction norms for flowering time, expressed as calendar days (Fig. 2A) or GDD (Fig. 2B), for all individuals and parents across the environmental gradient quantified by the population means of calendar days or GDD.

The general linear mixed-effects model (eqn1) revealed that at the whole design level and at the country level, all effects (Genotype, Environment, G×E) were significant (Supplementary Table S4). At this whole design level, the environment, the factor contributing most to phenotypic variance, was more important when flowering time was expressed as calendar days (Fig. 2C) rather than as GDD (Fig. 2D). The proportions of G×E and Genotype variances of flowering time increased substantially towards Southern environments (SP, for which a single year of study could be performed, was not included in this analysis). The G×E variance was further split into a most contributing Genotype by Location (GxL) term and a significant Genotype by Year interaction (G×Y) term (Supplementary Table S4).

By-site heritabilities for both calendar day and GDD were higher in Spain (H^2 = 0.94, 0.95), Italy (H^2 = 0.92, 0.89) and France (H^2 = 0.91, 0.88) than in Northern countries, Germany (H^2 = 0.59, 0.32) and Poland (H^2 = 0.40, 0.34) (Supplementary Table S5). In subsequent analyses, we have retained the data relating to the flowering period expressed in GDD, as they summarise the data with high efficiency by clearly identifying the heat demand of the plants for flowering, while the calendar days reflect a combination of multi environmental factors.

Plasticity parameters involved in G×E

For each model, AMMI, joint (FW) regression and factorial regression, analyses of variance revealed significant genotype, environment and G×E effects ($p < 0.001$) (Supplementary Tables S6, S7, S8). We further characterized G×E at the genotypic level with plasticity parameters derived from the three models (i.e., AMMI, FW and factorial regression) subsequently used for QTL mapping.

AMMI

Decomposition of the genotype-by-environment interaction through the AMMI model (Supplementary Table S6) showed a large number of significant IPCA values (from IPCA1 to IPCA9) ($p < 0.01$) using the F test of Gollob (1968). Each of these nine IPCA values explained from 4.3% to 21% of the variation in the SS_{GxE}, disclosing the complexity of the interaction patterns. The first two components captured less than half of the original variance (36.4%) with most of the environments poorly represented, complicating the interpretation of the biplots (Supplementary Fig. S2). The AMMI stability value (ASV) calculated on the first two IPCA ranged from 0.06 to 1.30 across the 109

366 individuals and the two parents (Fig. 3A, Supplementary Table S9). The genotypes 'H091', 'H0104'
367 and 'H077' had the lowest ASV values, while the genotypes 'H027', 'H073' and 'H122' had the highest
368 values.
369
370 *Joint regression (FW) and factorial regression analyses*
371 We considered the slopes of the joint regression (slope_FW) and the factorial regression models as
372 measures of individual plasticity (Figs 3B, C). While slope_FW was calculated by regressing the
373 observed phenotypes on the effects of the environment (Supplementary Table S10), the factorial
374 regression slope was calculated with different explicit environmental covariates (Malosetti et al.,
375 2013), which allowed us to assess the contribution of each climatic variable to G×E. Mean
376 temperature (Tmean) was the factor that contributed most to the interaction (Supplementary Table
377 S11), which is consistent with the use of GDD, which takes Tmean into account in its calculation.
378 Moreover, this contribution and that of the GDD were also the most significant when the factorial
379 regression analysis was carried out in calendar days (Supplementary Table S11). Other variables such
380 as photoperiod, photoperiod × GDD and global radiation did not improve the model (Supplementary
381 Table S11). Thus, we calculated the slope using Tmean as covariate (slope_Tmean) (Supplementary
382 Table S11). Notably, the use of Tmean as the environmental index was more efficient to model G×E,
383 as the factorial regression captured a larger variance of G×E (8.5%) than the FW regression (2.8%)
384 (Supplementary Tables S7, S8).
385 Individuals showed a wide range of slope (slope_FW, slope_Tmean) (Figs 3B, C; Supplementary Table
386 S12). Slopes from both models were highly negatively correlated (R^2 = 0.91) (Supplementary Fig.
387 S3A). They were also correlated to the overall mean flowering time (R^2 = 0.67) (Supplementary Figs
388 S3B, C), indicating that early flowering genotypes were on average less stable. Indeed, late genotypes
389 (e.g. 'H102') in Southern locations could rank as early or moderate early flowering genotypes in
390 Northern locations, whereas early flowering genotypes (e.g. 'H056') in Southern locations could rank
391 as moderately late or late flowering genotypes in Northern Europe (Figs 3B, C).
392 In addition, the joint regression model estimates a non-linear plasticity parameter, which presumably
393 has a different genetic basis (Kusmec et al., 2017). This parameter is the residual error of the joint
394 regression model (Fig. 3D). Several genotypes, namely 'H036', 'H120', 'H105', 'H064' and 'H065',
395 presented high residual variances as they displayed a nonlinear response to the environmental
396 gradient (Fig. 3D; Supplementary Table S10). For instance, 'H036' was overall ranked as a moderate
397 early flowering genotype but presented a large deviation in FR18, where it was the second earliest
398 genotype.
399
400 **Genetic architecture of flowering time**

We explored the genetic architecture of flowering time through QTL analysis based on male and female linkage maps with a total of 12196 SNP markers from the Affymetrix® SNP array (Hardigan et al., 2020). The linkage maps were constructed with a total of 6778 and 5418 markers for the female and male linkage maps, respectively. The final number of markers covered the expected 28 linkage groups (LG) for both female and male maps with additional small LG (44 for female and 33 for male linkage maps) (Supplementary Table S13). The lengths of the female and male linkage maps were 2298.5 cM and 1653.1 cM, respectively, with an average distance between markers of 0.7 cM. LG were assigned to one of the seven homoeologous groups (HG) according to the nomenclature of Hardigan et al. (2020) where letters refer to subgenomes (A, B, C, D) and using the Royal Royce genome for LG orientation.

The list of significant QTL and QEI for single and multi-environment models and for plasticity parameters is provided in Table 2. A total of 28 QTL and QEI linked to flowering time were detected and represented on the linkage groups (Fig. 4A). They can be summarized into 10 unique QTL including two QTL on LG7A (Figs 4A, B). Four flowering time QTL were detected only with single-environment means (7A_F, 7A_M) or only with plasticity parameters (4D_F, 6B_M). The multi-environments model allowed the detection of three QEI (2C_M, 3A_M and 6D_M) and six QTL linked to mean flowering times (1B_M, 1C_M, 2C_M, 3A_M, 6A_M and 6D_M) (Fig. 4C). It is noteworthy that the trend of the QTL effect was maintained whatever the environment but its magnitude could vary considerably from one environment to another (Fig. 4D).

As could be expected from the strong correlations (>0.7) between the overall mean of flowering time and plasticity parameters (Supplementary Fig. S3), we observed co-localizations between them for 3A_M, 6A_M and 6D_M QTL. Of notice, 6A_M QTL was detected in Germany for the two years and for one plasticity parameter (IPCA6). Only two QTL displayed both interaction with the environment and co-localization between the overall mean flowering time and plasticity parameters, being 3A_M and 6D_M QTL. The latest displayed the highest number of co-localizations and the highest LOD values, being detected for five environments and three plasticity parameters (slope_Tmean, IPCA1 and IPCA2) whereas 3A_M QTL was only detected for SP19 and slope_Tmean. The 7A_M QTL was detected only with single-environment means (FR18 and IT18) and one plasticity parameter (IPCA2) (Figs 4A, B, 5A; Table 2).

Two results suggest an effect of temperature on the 6D_M QTL: (i) QTL and QEI for the mean flowering times and slopes calculated using the Tmean as covariate (slope_Tmean) are co-located in 6D_M (Fig. 4A) and (ii) the effect decreases from the south to the north of Europe (Fig. 4D). Indeed, we observed that the allelic effect of 6D_M QTL increased linearly (R^2 = 0.80) with Tmean across

436 environments (Fig. 5A), resulting in a difference of up to 150 GDD (more than six days) in the
437 warmest environment (SP19) but less than 25 GDD (less than one day) in the coldest environment
438 (GE18) (Fig. 4D). Such relation was less clear for the other QEI (2C_M and 3A_M QTL, Supplementary
439 Fig. S4).
440 We focused more specifically on the effect of alleles associated with the three QTL, 6D_M, 6A_M and
441 3A_M co-localizing for the overall mean flowering times in the multi-environment model and
442 plasticity parameters (Fig. 5B). The single-marker analysis showed the strongest effect of the allele
443 linked to the 6D_M QTL on flowering time compared with the 3A_M and 6A_M, with a gain of
444 respectively 52, 30 and 35 GDD (Supplementary Fig. S5). The earliest flowering genotypes combined
445 the A alleles for the three markers while the latest flowering genotypes were H for the three markers
446 with an average gain of 97 GDD (Fig. 5B).
447
448 **Candidate genes**
449
450 We identified five candidate genes associated with flowering time within the common Bayesian
451 credible interval of 3A_M, 6A_M and 6D_M QTL (Table 3). We retained candidate genes when they
452 were annotated in both Camarosa va1.0 (Edger et al., 2019) and Royal Royce va1.0 (Hardigan et al.,
453 2021) genomes. In the LG3A_M interval, we identified two candidate genes associated with flowering
454 time: *FaCEN-like* (*CENTRORADIALIS*) and *FaFRI-like* (*FRIGIDA*). In the LG6A_M interval, we identified
455 two flowering-time-related proteins: FaFY and FaFPA. In the LG6D_M QTL interval *FaTFL1* (*TERMINAL*
456 *FLOWER1*, which belongs to the CENTRORADIALIS/TERMINAL FLOWER 1/SELF-PRUNING (CETS)
457 family, as *FaCEN-like* in LG3A_M, was the most relevant candidate gene.
458
459 **Development of a KASP marker for Marker Assisted Selection**
460
461 We developed a KASP marker linked to the 6D_M QTL (KASP_6D) for further use in Marker-Assisted
462 Selection (MAS) in breeding programs. We analyzed the polymorphism of this marker in our bi-
463 parental population. In addition, we validated its utilization by using a collection of 94 strawberry SF
464 genotypes scored in two successive years in France (Douville). This marker was able to discriminate
465 three genotypes: C/C, T/C, and T/T (Fig. 5C). In the bi-parental population, C/C genotypes required on
466 average 50 fewer heat units (GDD) than T/C genotypes and thus provided earlier flowering (Fig. 5D).
467 Its allelic effect was highest in Spain (a gain of up to 133 heat units (GDD) i.e. almost 8 days) and
468 lowest (a gain of 0-2 days) in Germany and Poland. T/T alleles were exclusively present in the
469 collection of SF genotypes where C/C alleles brought a gain of 73 heat units (GDD) (around 7 days)
470 compared to T/T. The phenotypes of the T/C and T/T genotypes were not significantly different (Fig.

5D). Overall, our results clearly indicate that the introduction of C/C alleles can be effective in the selection of early flowering strawberry varieties, especially in southern Europe.

Discussion

Flowering time has been extensively characterized in crop species as co-determinant of seed or fruit yield (Jung and Müller, 2009; Eshed and Lippman, 2019). The plasticity of flowering time has been well studied in crops (Li et al., 2018), but the variability of its response to various environmental cues depends on species and/or environmental range (Arnold et al., 2019). The genetic architecture of the plasticity, i.e. the ability of a plant to change its phenotype according to environments, has been investigated in a limited number of crop species (e.g., sorghum, Li et al., 2018; tomato, Diouf et al., 2020; maize, Jin et al., 2023; cherry, Branchereau et al., 2023). To date, no similar effort has been devoted to strawberry.

Here, thanks to a multi-European research program coordinated between five southern and northern European countries representative of the leading strawberry production areas in Europe, we have for the first time dissected the genetic basis of flowering time and its plasticity in relation to environmental cues. To this end, we analyzed the phenotypic response of a segregating population of cultivated strawberry grown in nine contrasting environments using different models. The genetic architecture highlighted both shared and distinct genetic control of flowering time and its plasticity, as well as genetic-based sensitivity to temperature variations.

The plasticity of flowering time is driven by temperature over a wide range of latitudes

Identifying environmental parameters that have an impact on flowering time is essential to understand the mechanisms underlying its phenotypic plasticity (Mu et al., 2022). Temperature and photoperiod are known as major drivers of this trait (Blackman, 2017). In our study, we showed the predominance of the temperature when modeling flowering time, with thermal time (GDD) having the highest efficiency (85%) when compared to photoperiod (62%) or global radiation (37%) (Table 1). The 15 percent remaining efficiency could be due to differences in cultural techniques among countries (e.g., soilless culture in France or soil culture in Italy), which produce different plant architectures and therefore variations in flowering patterns (Neri et al., 2012).

Plasticity can also be studied through the decomposition of G×E, which reveals the variation in reaction norms between genotypes (Sultan, 1987). We showed here that in strawberry, the G×E

506 variance for flowering time represents a high proportion of the total variance. This result indicates
507 that, when flowering time is considered, strawberry is a very plastic species, more so than suggested
508 for sorghum and cherry (Li et al., 2018; Branchereau et al., 2023). Among the models used for
509 studying G×E, the factorial regression models describe a genetically controlled differential sensitivity
510 to explicit environmental factors (Malosetti et al., 2013). These models, therefore, provide responses
511 as to the climatic drivers of the trait (Lombardi et al., 2022) and environmental indexes that can be
512 used to predict trait performance and inform the design of future studies (Guo et al., 2023). In our
513 study, the factorial regression model used confirmed results from the GDD model by identifying the
514 mean temperature as the dominant climatic factor affecting flowering time, well ahead of
515 photoperiod or global radiation (Supplementary Table S11).
516
517 The weaker influence of photoperiod than temperature on flowering time is likely due to the fact
518 that our study was conducted on a population of SF genotypes, the most common type of cultivated
519 strawberry. Photoperiod plays an essential role in floral initiation of strawberry (Heide et al., 2013).
520 In SF strawberry, the dormancy period separates floral initiation from flowering (Gaston et al., 2021)
521 and, therefore, can act as a reset, leading to at least partial independence between these two
522 processes (Krüger et al., 2022). In contrast, in PF strawberry i.e. varieties producing flowers all along
523 their vegetative cycle (Samad et al., 2022), and in forcing cultures with a year-round production
524 system (Yamasaki, 2013), floral initiation is immediately followed by flowering, which may explain
525 why photoperiod can have a greater influence on the timing of flowering.
526
527 **Improving the prediction of flowering time in contrasting environments**
528
529 In the very near future, strawberry production areas will face major variations in both average
530 temperature (Tmean) and maximum temperature (Tmax) as a result of climate change
531 (https://www.ipcc.ch/assessment-report/ar6/). To predict the adaptation of a strawberry variety to
532 various environments using modeling, the parameters of the model must be accurately determined.
533
534 To calculate heat accumulation, the GDD model assumes that there is a lower limit temperature (Tb).
535 In strawberry, Tb was imputed arbitrary for blooming at 0°C (Opstad et al., 2011; Bethere et al.,
536 2016) or was calculated for leaf appearance (0°C, Rosa et al., 2011). Our GDD model calculated Tb as
537 -1.7°C. Such negative Tb temperature has been previously described, for example in wheat for leaf
538 appearance (Zartash et al., 2020). Our calculated minimum temperature is thus consistent with the -
539 1.0 to -2.0°C temperatures of the cold rooms used to store plug plants and stop their development
540 until plantation (Lieten et al., 2005).

The GDD model does not predict the maximum temperature (Tmax), the temperature threshold above which additional heat no longer contributes to the calculation of flowering time (Elmendorf and Hollister, 2023). However, knowing the Tmax is necessary to anticipate the high temperatures predicted by climate change models. Using the triangular model, we estimated Tmax at 34°C; this temperature was exceeded only occasionally in our experiments. The Tb and Tmax values found in our study will be incorporated into models to improve flowering time prediction for strawberry, particularly under the hottest conditions (Jochner et al., 2016).

Integrating the results of the G×E analyses makes it possible to decipher the genetic architecture of flowering time plasticity

In the context of climate change, to overcome the problem of traditionally selected varieties, which are highly efficient but not very plastic, it is becoming increasingly necessary to produce genotypes suitable for multi environments. This can be achieved by taking advantage of phenotypic plasticity in breeding programs (Kusmec et al., 2018; Monforte, 2020). The genetic basis of phenotypic plasticity has been a central research topic in recent decades (Pigliucci, 2005). In this study, by combining the detection of multi-environmental and environment-specific QTL, we have highlighted the differential sensitivity of QTL to environmental changes and the influence of G×E on strawberry flowering phenotype. We observed four QTL displaying co-localization between the mean flowering times (single- and multi-environment models) and plasticity parameters (3A_M, 6A_M, 6D_M and 7A_M). Remarkably, while two of these QTL (3A_M and 6A_M) were identified in a single country (the 3A_M QTL in Spain, the 6A_M QTL in Germany), the 6D_M QTL was detected across multi environments and in the five countries. In the case of the 3A_M, 6A_M and 7A_M QTL, the genetic control of flowering time likely reflects the adaptation of strawberry to local climates (Mitchell-Olds and Schmitt, 2006). The 3A_M QTL could particularly be useful for breeding strawberry varieties adapted to the hotter conditions of Spain and other countries where strawberry production is expanding (for example Morocco and Mexico), whereas the use of the 6A_M QTL could be more relevant in temperate-cold conditions. The 7A_M QTL was a particular case as it was not detected in the multi-environment model and could be linked to specific conditions met in France and Italy in 2018. Remarkably, the sign of the effect of 6D_M QTL was consistent across all environments, meaning that it can be used in breeding programs to create varieties adapted to both northern and southern European climates. However, as its effect on flowering time is higher in southern (subtropical) Europe and lower in northern (temperate-cold) Europe, the use of this QTL for breeding would be more relevant in southern Europe and other countries with similar climates.

Two models have been proposed for the genetic control of phenotypic plasticity (Via et al., 1995): (i) the gene-regulation model, according to which regulatory loci modify the expression of other genes (e.g. structural genes) as a function of the environment, and (ii) the allelic sensitivity model, according to which the alleles underlying the QTL are differentially expressed depending on the environment. These models involve different genetic controls: the gene-regulation model implies that QTL for plasticity parameters are distinct from the mean flowering times QTL, whereas the allelic sensitivity model implies co-localization between them (Gutteling et al., 2007). For four QTL (3A_M, 6A_M, 6D_M and 7A_M), we found co-localization between the mean flowering times QTL and plasticity parameters QTL, which is typically expected for the allelic sensitivity model (Gutteling et al., 2007; Diouf et al., 2020). Most other QTL were either specific to the mean flowering times (e.g. 1B_M, 1C_M and 7A_F) or to one of the plasticity parameters (e.g. 4D_F and6B_M), which is consistent with the gene-regulation hypothesis. Therefore, in the population and environments studied, we found a co-occurrence of the two models in the genetic architecture of flowering time, which is consistent with previous reports on flowering time and other traits in other crop species (Lacaze et al., 2009; Gage et al., 2017; Kusmec et al., 2017; Diouf et al., 2020; Jin et al., 2023).

As cultivated strawberry is an octoploid species (Edger et al., 2019; Gaston et al., 2020), we may hypothesize that strawberry utilizes various homoeoalleles to regulate the timing of flowering depending on the environment, as previously proposed for the control of fruit quality traits (Lerceteau-Köhler et al., 2012). This polyploid plasticity has been postulated to play a considerable role in the evolution of polyploid crop species (Jackson and Chen, 2010). This hypothesis would have far-reaching implications in strawberry breeding as different homoeoalleles of a same gene carried by different chromosomes could contribute to the timing of flowering in changing environmental conditions. However, in strawberry, genomic redundancy does not necessarily translate into greater trait plasticity as previously shown by a study on the influence of polyploidy on the environmental fitness of a series of diploid and polyploid strawberry species (Wei et al., 2019).

TFL1, a likely candidate gene underlying the 6D_M QTL.

Several flowering-related genes could be found in the intervals of the three QTL (3A_M, 6A_M, and 6D_M) for which we observed co-localizations between the overall mean flowering times and plasticity parameters. Among these, 3A_M and 6D_M QTL are both sensitive to temperature. The *A. thaliana* homologous of *FaCEN-like* candidate gene underlying the 3A_M QTL has been shown to prolong vegetative growth and consequently delays flowering (Amaya et al., 1999). The *A. thaliana*

611 homolog of the *FaFRI-like* candidate gene that is also found in the 3A_M QTL encodes a transcription
612 factor that positively regulates the expression of *FLOWERING LOCUS C (FLC)* and plays a role in the
613 regulation of natural variation in flowering time in *A. thaliana* (Michaels et al., 2004). Interestingly,
614 Zhu et al. (2021) suggested that a temperature-controlled nuclear condensation mechanism
615 modulates the *FRI* activation of *FLC* transcription, thus contributing to the repression of flowering.
616 The *FaFY* and *FaFPA* candidate genes found in the 6A_M QTL are both known to play a role in *A.*
617 *thaliana* in the regulation of flowering time in the autonomous flowering pathway by acting on FLC
618 (Koornneef et al., 1991, Cheng et al., 2017).
619
620 The *FaTFL1* candidate gene underlying the LG6D_M QTL belongs to the CENTRORADIALIS/TERMINAL
621 FLOWER 1/SELF-PRUNING (CETS) family which plays a pivotal role in either activating or repressing
622 flowering (Wickland and Hanzawa, 2015). The role of TFL1 proteins as major floral repressors is
623 conserved in several species, including tomato (Pnueli et al., 1998) and strawberry (Iwata et al., 2012;
624 Nakano et al., 2015; Koskela et al., 2016). To date, in the diploid strawberry *Fragaria vesca*, the only
625 study on the genetic architecture of flowering time (Samad et al., 2017) was unable to highlight the
626 role of *FvTFL1* in the variation of this trait, as all the genotypes studied were *Fvtfl1* PF mutants.
627 However, *FvTFL1* probably plays a role in regulating the flowering time in *F. vesca*, as its expression is
628 regulated by temperature, being down-regulated at cool temperatures (<13°C) and up-regulated at
629 higher temperatures (23°C); moreover, these features are independent of photoperiod (Rantanen et
630 al., 2015). In cultivated strawberry, *FaTFL1* sensitivity to temperature has been shown to vary
631 according to the genotype: in 'Elsanta', *FaTFL1* expression was increased from 9°C to 21°C whereas
632 the temperature had no effect in 'Glima' (Koskela et al., 2016). We can assume that one of the two
633 *FaTFL1* homoeoalleles located in the LG6D_M QTL is expressed more in subtropical conditions where
634 temperatures are higher; consequently, this *FaTFL1* allele would delay flowering more significantly in
635 subtropical conditions than in cold temperature conditions. Future studies in controlled conditions
636 will test this hypothesis, for example by carrying out a RNAseq analysis of plant tissues (leaf and bud)
637 collected from genotypes carrying different *FaTFL1* alleles and grown at different temperatures.
638
639 **Conclusion**
640 In the context of climate change, it is necessary to uncover the genetic architecture of the plasticity
641 of complex traits in cultivated species. Here, in a concerted European effort, we studied flowering
642 time, a trait that is highly sensitive to the environment, and showed that temperature is the most
643 significant driver of this trait in cultivated strawberry. The detection of several QTL and the
644 identification of underlying candidate genes associated with flowering time plasticity will help to
645 better understand the molecular mechanisms responsible for variations in flowering time and select

646 superior strawberry varieties that are well suited to changing environmental conditions. To this end,
647 we designed the breeder-friendly genetic marker KASP_6D for a major temperature-sensitive QTL,
648 which will accelerate MAS selection for flowering time in cultivated strawberry. Our study will have
649 far-reaching implications for the selection of new strawberry varieties adapted not only to the wide
650 differences in climatic conditions found in Europe, but also to countries with tropical/sub-tropical
651 climates where strawberry production is expanding rapidly.
652

Acknowledgements. The authors thank Philippe Chartier, Cédric Duranton and Christian Gauthier (Invenio), Luis Miranda and José A. Gómez-Mora (IFAPA) for strawberry culture and phenotyping. The authors thank Drs. Isidore Diouf and Iñaki Garcia de Cortazar Atauri for fruitful discussions.

Authors contributions

KO chose the cross 'Candonga' × 'Senga Sengana' and produced the 1st generation of individuals; BD and members of the GoodBerry project conceived and designed the experiments. AleP and BD analyzed and interpreted the data; BD and AleP wrote the manuscript and CR contributed to the writing of the manuscript. All authors discussed the results and commented on the manuscript.

Conflict of interest. No conflict of interest declared.

Funding. The project was funded by European Union's Horizon 2020 research and innovation program (BreedingValue project N° 101000747). AleP PhD has been supported by Invenio and the Association Nationale de la Recherche et la Technologie (ANRT) (Cifre agreement).

Data availability.

Data will be made available on request.

Supplementary data

Supplementary Figures

Supplementary Figure S1. Culture workflow of the European Goodberry project.

Supplementary Figure S2. Biplots of the first three components of AMMI analysis of flowering time.

Supplementary Figure S3. Relationship between GDD, slope_FW and slope_Tmean.

Supplementary Figure S4. Relationship between the QTL effect expressed in GDD and the temperature.

Supplementary Figure S5. Single marker analysis showing the effect of the Affymetrix® allele linked to the flowering time QTL.

688

689

690 **Supplementary Tables**

691

692 Supplementary Table S1. Name and sequence of primers used for the validation of the 6D_M QTL.
693 Tm, annealing temperature.

694

695 Supplementary Table S2. Descriptions of the nine environments.

696

697 Supplementary Table S3. Spearman phenotypic correlations for flowering time between
698 environments.

699

700 Supplementary Table S4. ANOVA with mixed model, where genotype and genotype-environment
701 interaction (G×E) are random effects.

702

703 Supplementary Table S5. Broad-sense heritabilities (H2) of flowering time by environment, country
704 and whole-design level.

705

706 Supplementary Table S6. ANOVA for Additive Main Effects and Multiplicative Interaction (AMMI)
707 model applied to flowering time (GDD) in the segregating population 'Candonga' x 'Senga Sengana'
708 under nine environments.

709

710 Supplementary Table S7. ANOVA using joint regression (FW) model on flowering time expressed in
711 GDD.

712

713 Supplementary Table S8. ANOVA using factorial regression model on flowering time expressed in
714 GDD or in calendar day.

715

716 Supplementary Table S9. AMMI Stability Value (ASV) calculated on the first two ICPA for flowering
717 time (GDD).

718

719 Supplementary Table S10. Linear (slope_FW) and non-linear (residual variance, VAR_FW) plasticity.

720

721 Supplementary Table S11. Factorial regression models incorporating environmental information as
722 covariate.

Supplementary Table S12. Linear (slope_Tmean) plasticity provided by the factorial regression model on Tmean.

Supplementary Table S13. Summary of the linkage maps of the segregating population 'Candonga' x 'Senga Sengana'.

References

Amaya I, Ratcliffe OJ, Bradley DJ. 1999. Expression of CENTRORADIALIS (CEN) and CEN-like genes in tobacco reveals a conserved mechanism controlling phase change in diverse species. The Plant Cell 11:1405-1418. doi: 10.1105/tpc.11.8.1405.

Arnold PA, Kruuk LEB, Nicotra AB. 2019. How to analyse plant phenotypic plasticity in response to a changing climate. New Phytologist 222:1235-1241. doi: 10.1111/nph.15656.

Bakare MA, Kayondo SI, Aghogho CI, Wolfe MD, Parkes EY, Kulakow P, Egesi C, Rabbi IY, Jannink JL. 2022. Exploring genotype by environment interaction on cassava yield and yield related traits using classical statistical methods. PLoS One 17:e0268189. doi: 10.1371/journal.pone.0268189.

Bates D, Maechler M, Bolker B, Walker S. 2021. lme4: Linear Mixed-Effects Models using Eigen and S4. R package version 1.1-27.1, URL https://CRAN.R-project.org/package=lme4.

Bates D, Mächler M, Bolker B, Walker S. 2015. Fitting Linear Mixed-Effects Models Using lme4. Journal of Statistical Software 67:1–48. https://doi.org/10.18637/jss.v067.i01

Bethere L, Sīle T, Seņņikovs J, Bethers U. 2016. Impact of climate change on the timing of strawberry phenological processes in the Baltic States. Estonian Journal of Earth Sciences 65:48–58. doi: 10.3176/earth.2016.04.

Blackman BK. 2017. Changing Responses to Changing Seasons: Natural Variation in the Plasticity of Flowering Time. Plant Physiology 173:16-26. doi: 10.1104/pp.16.01683.

Branchereau C, Hardner C, Dirlewanger E, Wenden B, Le Dantec L, Alletru D, Parmentier J, Ivančič A, Giovannini D, Brandi F, Lopez-Ortega G, Garcia-Montiel F, Quilot-Turion B, Quero-García J. 2023. Genotype-by-environment and QTL-by-environment interactions in sweet cherry (Prunus avium L.) for flowering date. Frontiers in Plant Science 14:1142974. doi: 10.3389/fpls.2023.1142974.

Broman KW, Wu H, Sen S, Churchill GA. 2003. R/qtl: QTL mapping in experimental crosses. Bioinformatics 19:889–890. doi: 10.1093/bioinformatics/btg112.

Ceccarelli S. 1989. Wide adaptation: how wide? Euphytica 40:197–205. https://doi.org/10.1007/BF00024512.

Cheng JZ, Zhou YP, Lv TX, Xie CP, Tian CE. 2017. Research progress on the autonomous flowering time pathway in Arabidopsis. Physiology and Molecular Biology of Plants. 23:477-485. doi: 10.1007/s12298-017-0458-3.

Cho LH, Yoon J, An G. 2017. The control of flowering time by environmental factors. The Plant Journal 90:708-719. doi: 10.1111/tpj.13461.

Chuine I, Cour P, Rousseau DD. 1998. Fitting models predicting dates of flowering of temperate zone trees using simulated annealing. Plant, Cell & Environment 21:455–466.

Chuine I, De Cortazar-Atauri IG, Kramer K, Hänninen H. 2013. Plant development models. Phenology: An Integrative Environmental Science. Springer, pp. 275–293.

Diouf I, Derivot L, Koussevitzky S, Carretero Y, Bitton F, Moreau L, Causse M. 2020. Genetic basis of phenotypic plasticity and genotype × environment interactions in a multi-parental tomato population. Journal of Experimental Botany 71:5365-5376. doi: 10.1093/jxb/eraa265.

Edger, P. P., Poorten, T. J., VanBuren, R., et al. 2019. Origin and evolution of the octoploid strawberry genome. Nature Genetics 51:541–547. https://doi.org/10.1038/s41588-019-0356-4.

Elmendorf SC, Hollister RD. 2023. Limits on phenological response to high temperature in the Arctic. Scientific Report 13:208. doi: 10.1038/s41598-022-26955-9.

Eshed Y, Lippman ZB. 2019. Revolutions in agriculture chart a course for targeted breeding of old and new crops. Science 366:eaax0025. doi:10.1126/science.aax0025

Finlay WK, Wilkinson GN. 1963. The analysis of adaptation in a plant breeding program. Australian Journal of Agricultural Research 14:742–754.

Gage JL, Jarquin D, Romay C, et al. 2017. The effect of artificial selection on phenotypic plasticity in maize. Nature Communications 8:1348. doi:10.1038/s41467-017-01450-2.

Gaston A, Osorio S, Denoyes B, Rothan C. 2020. Applying the Solanaceae Strategies to Strawberry Crop Improvement. Trends in Plant Science 25:130-140. doi: 10.1016/j.tplants.2019.10.003.

Gaston A, Potier A, Alonso M, et al. 2021. The FveFT2 florigen/FveTFL1 antiflorigen balance is critical for the control of seasonal flowering in strawberry while FveFT3 modulates axillary meristem fate and yield. New Phytologist 232:372-387. doi: 10.1111/nph.17557.

Gauch HG. 2013. A Simple Protocol for AMMI Analysis of Yield Trials. Crop Science 53: 1860-1869. https://doi.org/10.2135/cropsci2013.04.0241.

Gollob HF. 1968. A statistical model which combines features of factor analytic and analysis of variance techniques. Psychometrika 33:73-115. doi: 10.1007/BF02289676.

Guo T, Wei J, Li X, Yu J. 2023. Environmental context of phenotypic plasticity in flowering time in sorghum and rice. Journal of Experimental Botany erad398. https://doi.org/10.1093/jxb/erad398.

Gutteling EW, Riksen JA, Bakker J, Kammenga JE. 2007. Mapping phenotypic plasticity and genotype-environment interactions affecting life-history traits in Caenorhabditis elegans. Heredity (Edinb). 98:28-37. doi: 10.1038/sj.hdy.6800894.

Hänninen H. 1990a. Modeling dormancy release in trees from cool and temperate regions. pp:159-165 in R. K. Dixon, R. S. Meldahl, G. A. Ruark, and W. G. Warren, editors. Process modeling of forest growth responses to environmental stress. Timber Press, Portland.

Hänninen H. 1990b. Modelling bud dormancy release in trees from cool and temperate regions. Acta Forestalia Fennica 213:1-47. https://doi.org/10.14214/aff.7660.

Hardigan MA, Feldmann MJ, Lorant A, Bird KA, Famula R, Acharya C, Cole G, Edger PP, Knapp SJ. 2020. Genome Synteny Has Been Conserved Among the Octoploid Progenitors of Cultivated Strawberry Over Millions of Years of Evolution. Frontiers in Plant Science 10:1789. https://doi.org/10.3389/fpls.2019.01789.

Hardigan MA, Feldmann MJ, Pincot DDA et al. 2021. Blueprint for Phasing and Assembling the Genomes of Heterozygous Polyploids: Application to the Octoploid Genome of Strawberry. bioRxiv doi: https://doi.org/10.1101/2021.11.03.467115.

Heide OM, Stavang JA, Sønsteby A. 2013. Physiology and genetics of flowering in cultivated and wild strawberries - a review. Journal of Horticultural Science & Biotechnology 88:1-18. https://doi.org/10.1080/14620316.2013.11512930.

Iwata H, Gaston A, Remay A, Thouroude T, Jeauffre J, Kawamura K, Oyant LHS, Araki T, Denoyes B, Foucher F. 2012. The TFL1 homologue KSN is a regulator of continuous flowering in rose and strawberry. The Plant Journal 69:116-125. doi: 10.1111/j.1365-313X.2011.04776.x.

Jackson S, Chen ZJ. 2010. Genomic and expression plasticity of polyploidy. Current opinion in plant biology 13:153–159. https://doi.org/10.1016/j.pbi.2009.11.004.

Jin M, Liu H, Liu X, et al. 2023. Complex genetic architecture underlying the plasticity of maize agronomic traits. Plant Communications 4:100473. doi: 10.1016/j.xplc.2022.100473.

Jochner S, Sparks TH, Laube J, Menzel A. 2016. Can we detect a nonlinear response to temperature in European plant phenology? International Journal of Biometeorology 60:1551-1561. doi: 10.1007/s00484-016-1146-7.

Jung C, Müller AE. 2009. Flowering time control and applications in plant breeding. Trends in Plant Science 14:563-573. doi: 10.1016/j.tplants.2009.07.005.

Koembuoy K, Hasegawa S, Otagaki S, Takahashi H, Nagano S, Isobe S, Shiratake K, Matsumoto S. 2020. RNA-seq Analysis of Meristem Cells Identifies the FaFT3 Gene as a Common Floral Inducer in Japanese Cultivated Strawberry. Horticulture Journal 89:138-146.

Koornneef M, Hanhart CJ, van der Veen JH. 1991. A genetic and physiological analysis of late flowering mutants in Arabidopsis thaliana. Molecular Genetics and Genomics 229:57-66. doi: 10.1007/BF00264213.

Koskela EA, Mouhu K, Albani MC, Kurokura T, Rantanen M, Sargent DJ, Battey NH, Coupland G, Elomaa P, Hytönen T. 2012. Mutation in TERMINAL FLOWER1 reverses the photoperiodic requirement for flowering in the wild strawberry Fragaria vesca. Plant Physiology 159:1043-1054. doi: 10.1104/pp.112.196659.

Koskela EA, Sønsteby A, Flachowsky H, Heide OM, Hanke MV, Elomaa P, Hytönen T. 2016. TERMINAL FLOWER1 is a breeding target for a novel everbearing trait and tailored flowering responses in cultivated strawberry (Fragaria × ananassa Duch.). Plant Biotechnology Journal 14:1852-1861. doi: 10.1111/pbi.12545.

Krüger E, Woznicki TL, Heide OM, et al. 2022. Flowering Phenology of Six Seasonal-Flowering Strawberry Cultivars in a Coordinated European Study. Horticulturae 8:933. https://doi.org/10.3390/horticulturae8100933.

Kusmec A, de Leon N, Schnable PS. 2018. Harnessing Phenotypic Plasticity to Improve Maize Yields. Frontiers in Plant Science 9:1377. doi: 10.3389/fpls.2018.01377.

Kusmec A, Srinivasan S, Nettleton D, Schnable PS. 2017. Distinct genetic architectures for phenotype means and plasticities in Zea mays. Nature Plants 3:715-723. doi: 10.1038/s41477-017-0007-7.

Labadie M, Vallin G, Potier A, Petit A, et al. 2022. High Resolution Quantitative Trait Locus Mapping and Whole Genome Sequencing Enable the Design of an Anthocyanidin Reductase-Specific Homoeo-Allelic Marker for Fruit Colour Improvement in Octoploid Strawberry (Fragaria × ananassa). Frontiers in Plant Science 13: 869655 https://dx.doi.org/10.3389/fpls.2022.869655.

Lacaze X, Hayes PM, Korol A. 2009. Genetics of phenotypic plasticity: QTL analysis in barley, Hordeum vulgare. Heredity 102:163-173. doi:10.1038/hdy.2008.76.

Le Mière P, Hadley P, Darby J, Battey NH. 1998. The effect of thermal environment, planting date and crown size on growth, development and yield of Fragaria x ananassa Duch. cv. Elsanta. The Journal of Horticultural Science and Biotechnology 73:786–795. https://doi.org/10.1080/14620316.1998.11511049.

Lerceteau-Köhler, E., Moing, A., Guérin, G., Renaud, C., Petit, A., Rothan, C., Denoyes B. 2012. Genetic 699 dissection of fruit quality traits in the octoploid cultivated strawberry highlights the role of homoeo-QTL in their control. Theoretical and Applied Genetics 124:1059–1077. https://doi.org/10.1007/s00122-011-1769-3.

Li X, Guo T, Mu Q, Li X, Yu J. 2018. Genomic and environmental determinants and their interplay underlying phenotypic plasticity. Proceedings of the National Academy of Sciences 115:6679-6684. doi: 10.1073/pnas.1718326115.

Li Y, Suontama M, Burdon RD, Dungey HS. 2017. Genotype by environment interactions in forest tree breeding: review of methodology and perspectives on research and application. Tree Genetics & Genomes 13-60. DOI 10.1007/s11295-017-1144-x.

Lieten P, Evenhuis B, Baruzzi G. 2005. Cold Storage of Strawberry Plants. International Journal of Fruit Science 5:75-82. DOI: 10.1300/J492v05n01_07.

Lombardi E, Shestakova TA, Santini F, Resco de Dios V, Voltas J. 2022. Harnessing tree-ring phenotypes to disentangle gene by environment interactions and their climate dependencies in a circum-Mediterranean pine. Annals of Botany 130:509-523. doi: 10.1093/aob/mcac092.

Malosetti M, Ribaut JM, van Eeuwijk FA. 2013. The statistical analysis of multi-environment data: modeling genotype-by-environment interaction and its genetic basis. Frontiers in Physiology 4:44. doi: 10.3389/fphys.2013.00044.

Michaels SD, Bezerra IC, Amasino RM. 2004. FRIGIDA-related genes are required for the winter-annual habit in Arabidopsis. Proceedings of the National Academy of Sciences 101:3281-3285. doi: 10.1073/pnas.0306778101.

Mitchell-Olds T, Schmitt J. 2006. Genetic mechanisms and evolutionary significance of natural variation in Arabidopsis. Nature. 441:947-952. doi: 10.1038/nature04878.

Monforte AJ. 2020. Time to exploit phenotypic plasticity. Journal of Experimental Botany 71:5295-5297. doi: 10.1093/jxb/eraa268.

Mu Q, Guo T, Li X, Yu J. 2022. Phenotypic plasticity in plant height shaped by interaction between genetic loci and diurnal temperature range. New Phytologist 233:1768-1779. doi: 10.1111/nph.17904.

Muñoz-Avila JC, Prieto C, Sánchez-Sevilla JF, Amaya I, Castillejo C. 2022. Role of FaSOC1 and FaCO in the seasonal control of reproductive and vegetative development in the perennial crop Fragaria × ananassa. Frontiers in Plant Science 13:971846.

Nakano Y, Higuchi Y, Yoshida Y, Hisamatsu T. 2015. Environmental responses of the FT/TFL1 gene family and their involvement in flower induction in Fragaria × ananassa. Journal of Plant Physiology 177:60-66. doi: 10.1016/j.jplph.2015.01.007.

Neri D, Baruzzi G, Massetani F, Faedi W. 2012. Strawberry production in forced and protected culture in Europe as a response to climate change. Canadian Journal of Plant Science 92: 1021-1036. https://doi.org/10.4141/cjps2011-276.

Opstad N, Sønsteby A, Myrheim U, Heide OM. 2011. Seasonal timing of floral initiation in strawberry: effects of cultivar and geographic location. Scientia Horticulturae 129:127–134. DOI:10.1016/j.scienta.2011.03.022.

Pigliucci M. 2005. Evolution of phenotypic plasticity: where are we going now? Trends in Ecology & Evolution 20:481–486.

Pnueli L, Carmel-Goren L, Hareven D, Gutfinger T, Alvarez J, Ganal M, Zamir D, Lifschitz E. 1998. The SELF-PRUNING gene of tomato regulates vegetative to reproductive switching of sympodial meristems and is the ortholog of CEN and TFL1. Development. 125:1979-89. doi: 10.1242/dev.125.11.1979.

Purchase J. 1997. Parametric analysis to describe genotype by environment interaction and yield stability in winter wheat. PhD Thesis 83–83. http://hdl.handle.net/11660/1966.

Rantanen M, Kurokura T, Jiang P, Mouhu K, Hytönen T. 2015. Strawberry homologue of terminal flower1 integrates photoperiod and temperature signals to inhibit flowering. The Plant Journal 82:163-73. doi: 10.1111/tpj.12809.

Rosa HT, Walter LC, Streck NA, Andriolo JL, Silva MR, Langner JA. 2011. Base temperature for leaf appearance and phyllochron of selected strawberry cultivars in a subtropical environment. Bragantia 70: 939–945. https://doi.org/10.1590/S0006-87052011000400029.

Rousseau-Gueutin M, Lerceteau-Köhler E, Barrot L, Sargent DJ, Monfort A, Simpson D, Arús P, Guérin G, Denoyes-Rothan B. 2008. Comparative genetic mapping between octoploid and diploid Fragaria species reveals a high level of colinearity between their genomes and the essentially disomic behavior of the cultivated octoploid strawberry. Genetics, 179:2045–2060. https://doi.org/10.1534/genetics.107.083840.

Samad S, Kurokura T, Koskela E, Toivainen T, Patel V, Mouhu K, Sargent DJ, Hytönen T. 2017. Additive QTLs on three chromosomes control flowering time in woodland strawberry (Fragaria vesca L.). Horticulture Research 4:17020. doi: 10.1038/hortres.2017.20.

Samad S, Rivero R, Kalyandurg PB, Vetukuri RR, Heide OM, Sønsteby A, Khalil S. 2022. Characterization of Environmental Effects on Flowering and Plant Architecture in an Everbearing Strawberry F1-Hybrid by Meristem Dissection and Gene Expression Analysis. Horticulturae 8:626. https://doi.org/10.3390/horticulturae8070626.

Senger E, Osorio S, Olbricht K, et al. 2022. Towards smart and sustainable development of modern berry cultivars in Europe. The Plant Journal 111:1238 – 1251. DOI:10.1111/tpj.15876.

Smith SM, Maughan PJ. 2015. SNP genotyping using KASPar assays. Methods in molecular biology. 1245:243-256. doi:10.1007/978-1-4939-1966-6_18.

Sønsteby A, Heide OM. 2007. Quantitative long-day flowering response in the perpetual-flowering F1 strawberry cultivar Elan. The Journal of Horticultural Science and Biotechnology. 82:266-274. doi: 10.1080/14620316.2007.11512228.

Sultan SE. 1987. Evolutionary Implications of Phenotypic Plasticity in Plants. In: Hecht, M.K., Wallace, B., Prance, G.T. (eds) Evolutionary Biology. Springer, Boston, MA. https://doi.org/10.1007/978-1-4615-6986-2_7.

Van Ooijen JW. 2011. Multipoint maximum likelihood mapping in a fullsib family of an outbreeding species. Genetics Research 93:343–349. doi: 10.1017/S0016672311000279.

Via S, Gomulkiewicz R, De Jong G, Scheiner SM, Schlichting CD, Van Tienderen PH. 1995. Adaptive phenotypic plasticity: consensus and controversy. Trends in Ecology & Evolution. 10:212-217. doi: 10.1016/s0169-5347(00)89061-8.

Voorrips, R.E. 2002. MapChart: software for the graphical presentation of linkage maps and QTLs. Journal of Heredity 93: 77-78. https://doi.org/10.1093/jhered/93.1.77

Wang E, Engel T. 1998. Simulation of Phenological Development of Wheat Crops. Agricultural Systems 58:1-24. doi:10.1016/S0308-521X(98)00028-6.

Wei N, Cronn R, Liston A, Ashman TL. 2019. Functional trait divergence and trait plasticity confer polyploid advantage in heterogeneous environments. New Phytologist 221:2286-2297. doi:10.1111/nph.15508.

Wickland DP, Hanzawa Y. 2015. The FLOWERING LOCUS T/TERMINAL FLOWER 1 Gene Family: Functional Evolution and Molecular Mechanisms. Molecular Plant 8:983-997. doi: 10.1016/j.molp.2015.01.007.

Yamasaki A. 2013. Recent Progress of Strawberry Year-round Production Technology in Japan, Japan Agricultural Research Quarterly 47:37-42. https://doi.org/10.6090/jarq.47.37.

Zartash F, Mukhtar A, Mubshar H, Ghulam A, Sami UA, Shakeel A, Niaz A, Muhammad AA, Ghulam S, Ehsan UH, Pakeeza I, Sajjad H. 2020. The fingerprints of climate warming on cereal crops phenology and adaptation options. Scientific Reports 10:18013. doi: 10.1038/s41598-020-74740-3.

Zhu P, Lister C, Dean C. 2021. Cold-induced Arabidopsis FRIGIDA nuclear condensates for FLC repression. Nature 599:657-661. doi: 10.1038/s41586-021-04062-5.

Tables

Table 1. Models for predicting flowering date as a function of temperature, photoperiod and/or global radiation: GDD, Triangular, Sigmoid, Wang. For photoperiod and global radiation, calculation of the GDD and triangular models were adapted to these two climatic parameters. Efficiency, ratio (SStot-SSres/SStot); RMSE, root mean squared error; t0, starting date in calendar day; SStar, sum calculated by the model from t0; Nobs, number of observations; Tb, base temperature; Tmin, minimum temperature; Topt, optimum temperature; Tmax, maximum temperature; PPmin, PPopt, PPmax or GRmin, GRopt, GRmax for minimum, optimum, maximum of photoperiod or global radiation; Temperatures and global radiations are expressed in °C and Watt/m2 respectively. Models were calculated with the PMP5 software (http://www.cefe.cnrs.fr/fr/recherche/ef/forecast/phenology-modelling-platform). Parameters of the models were adapted to the range of values of the climatic factors, Tmean (Tm), Global radiation (GR) or Phtoperiod (PP). d and e are Sigmoid model parameters.

Model	Efficiency (%)	RMSE	t0	SStar	Nobs	Tb_Tmin / PPmin / RGmin	Topt / PPopt / RGopt	Tmax or PPmax / RGmax	d	e
Simple model										
Temperature										
GDD:Tm	0.85	9.07	1	824.7	918	-1.7				
Triangular:Tm	0.85	9.07	1	31.7	918	-1.8	24.4	34.1		
Sigmoid:Tm	0.85	9.00	1	31.4	918				-0.19	11.32
Wang:Tm	0.85	9.00	1	30.4	918	-13.6	25.0	34.3		
Photoperiod										
GDD:PP	0.37	18.63	1	237.2	918	8.0				
Triangular:PP	0.62	14.47	1	47.50	918	7.8	12.10	14.09		
Global Radiation										
GDD:RG	0.07	22.59	66	12482	918	749.7				
Triangular:RG	0.68	13.06	1	50.8	918	141.9	888.9	2681.2		
Multiplicative models										
GDD:Tm and Triangular:PP	0.85	9.05	1	528.5	918	0.2	13.2	24		
GDD:Tm and Triangular:RG	0.79	11.00	16	198.7	918	0.5	1615	2470		

Table 2. QTL and QEI detected for flowering time in single and multi-environment models and for plasticity parameters. Chr, chromosome; Pos, genetic position in cM; ci_lo, lower genetic position in cM of the Bayesian credible interval; ci_hi, upper genetic position in cM of the Bayesian credible interval; LOD, logarithm of the odds ratio; a, mean phenotypic difference between the two homozygous loci of the QTL; r^2, percentage of total phenotypic variance explained by the QTL; QEI, QTL-by-Environment Interaction.

									QTL				QEI	
Environmnent (country and year) / parameter		Map	Marker	Chr	QTL name	Pos (cM)	ci_lo (cM)	ci_hi (cM)	LOD	a	r^2	p-value	LOD QEI	*p*-value
Single environment model for flowering time in GDD														
Spain	2019	M	AX-184271717	3A	3A_M	35.7	32.0	42.0	4.3	118.4	14.4	0.00	-	-
	2019	M	AX-184039651	6D	6D_M	12.7	8.2	18.0	7.1	148.6	24.0	0.00	-	-
Italy	2018	M	AX-184685694	6D	6D_M	9.1	4.0	14.0	4.7	79.0	17.9	0.00	-	-
	2018	M	c7A.loc28	7A	7A_M	28.0	14.0	38.0	3.7	56.3	9.0	0.00	-	-
	2019	F	AX-184654928	7A	7A_F	37.5	36.0	43.9	3.6	68.4	15.3	0.01	-	-
France	2018	M	AX-184265643	6D	6D_M	7.3	2.8	14.0	4.7	92.2	13.4	0.00	-	-
	2018	M	AX-184213081	7A	7A_M	21.9	12.1	39.1	2.9	85.5	11.6	0.07	-	-
Germany	2018	M	AX-184558831	6A	6A_M	61.2	50.0	62.0	3.3	22.6	16.2	0.03	-	-
	2018	M	AX-184857914	6D	6D_M	7.3	0.0	14.6	3.3	19.9	13.0	0.03	-	-
	2019	M	AX-184019931	6A	6A_M	54.0	48.5	60.0	3.6	42.5	14.3	0.02	-	-
Poland	2019	M	AX-184774131	6D	6D_M	18.2	12.7	23.6	3.4	32.9	13.5	0.02	-	-
Plasticity parameters														

SlopeTm	M	AX-184283141	3A	3A_M	21.2	16.0	26.7	3.6	9.6	12.3	0.02	-	-
SlopeTm	M	AX-184019970	6D	6D_M	12.7	5.5	16.0	7.8	13.5	26.3	0.00	-	-
lPCA1	M	AX-184492105	6D	6D_M	14.6	9.1	20.0	3.8	2.8	15.9	0.01	-	-
lPCA2	M	AX-184862361	6D	6D_M	8.2	2.8	14.0	3.8	2.6	16.0	0.01	-	-
lPCA2	M	AX-184213081	7A	7A_M	21.9	14.0	39.1	3.4	2.1	10.4	0.03	-	-
lPCA4	F	AX-184922666	4D	4D_F	27.2	22.0	34.0	3.0	1.6	13.0	0.04	-	-
lPCA6	M	AX-166507632	6A	6A_M	52.2	46.7	57.6	3.2	1.3	13.8	0.03	-	-
lPCA7	M	AX-184122477	6B	6B_M	39.6	33.3	44.0	3.6	0.5	15.3	0.01	-	-
Multi-environment model													
	M	AX-184561564	1B	1B_M	42.1	37.5	54.8	4.0	7.5	1.3	0.04	-	ns
	M	AX-184623363	1C	1C_M	17.2	7.3	25.4	4.3	29.9	1.5	0.02	-	ns
	M	AX-184291002	2C	2C_M	13.8	8.3	14.7	6.4	31.5	1.7	0.00	2.1	0.05
	M	c3A.loc20	3A	3A_M	20	11.8	76.2	5.6	33.1	1.4	0.00	2.1	0.05
	M	AX-184872554	6A	6A_M	57.6	54.0	80.0	6.8	35.3	2.3	0.00	-	ns
	M	AX-184254843	6D	6D_M	10.9	7.3	14.6	15.2	28.7	4.2	0.00	4.7	0

Table 3. Candidate genes identified in the three flowering time QTL common to the overall mean flowering times (multi-environment model) and the plasticity parameters.

QTL position	Position on Camarosa genome	Position on Royal Royce genome	Candidate gene	ID on Camarosa genome	ID on Royal Royce genome	Corresponding ID on diploid genome	Arabidopsis
LG3A	9077738-21022370	9867318-22377776	*CEN-like/ATC*	FxaC_9g27230	Fxa3Ag102363	FvH4_3g24700	AT2G27550
			FRI-like1	FxaC_9g28150	Fxa3Ag102288	FvH4_3g24000	AT5G16320
LG6A	7331233-11484453	24040354-27479667	*FY-like*	FxaC_21g17390	Fxa6Ag103856	FvH4_6g22190	AT5G13480
			FPA-like	FxaC_21g17211	Fxa6Ag103868	FvH4_6g40190	AT4G12640
LG6D	11903312-15757612	9377205-13301702	*TFL1*	FxaC_24g24110	Fxa6Dg101555	FvH4_6g18480	AT5G03840

Figure legends

Figure 1. Environment description and flowering time of the 'Candonga' x 'Senga Sengana' segregating population in nine environments.

(A) Location and latitudes of the five countries in which experimental trials were carried out.

(B) Clustering of the nine experimental environments according to the six environmental covariates measured from the 1st of January until end of flowering.

(C) Three genotypes, 'Candonga', 'Senga Sengana' and 'H062' under three environments in 2018 (France, Spain and Germany).

(D) Box plots showing the flowering time (calendar days) for the nine environments.

(E) Pairwise Spearman correlation values (r) between flowering time (calendar days) in the nine environments. The r values are represented by coloured circles whose size varies according to their value. Crossed-out circles indicate non-significant correlations (p-value > 0.05).

SP, Spain, IT, Italy, FR, France, GE, Germany, PL, Poland. 2018 and 2019 (18 and 19 respectively), years of experimentations. Sites are ordered by increasing order of latitude.

Figure 2. Reaction norms and analyses of variance for flowering time.

(A-B) Reaction norm for flowering time expressed in calendar days (A) or Growing Degree-Days (GDD) (B). The nine environments are ranked in increasing order of flowering time. Each line connects the flowering time values of individuals across environments. Red and blue lines represent 'Candonga' and 'Senga Sengana' respectively.

(C-D) Variance partitioning of flowering time (calendar days (C) and GDD (D)) by the linear mixed model for the nine environments or for each country.

SP, Spain, IT, Italy, FR, France, GE, Germany, PL, Poland. 2018 and 2019 (18 and 19 respectively), years of experimentations.

Figure 3. Distributions of plasticity parameters for all individuals and parents in the segregating population for flowering time.

(A) Histogram distribution of AMMI Stability Values (ASV) calculated for each genotype as the relative influence of IPCA1 and IPCA2 scores based on the sum of squares of their interaction.

(B-C) Slopes with Finlay–Wilkinson and factorial regression models for flowering time (GDD). Regressions of phenotypic performances of genotypes on environmental index (B) or on mean temperature (C). 'Candonga', 'Senga Sengana', 'H102' (example of a late flowering genotype) and 'H056' (example of an early flowering genotype) are plotted as red, blue, purple and orange lines, respectively.

SP, Spain, IT, Italy, FR, France, GE, Germany, PL, Poland. 2018 and 2019 (18 and 19 respectively), years of experimentations.

Figure 4. Effects of flowering time QTL and QTL-by-Environment Interactions (QEI).

(A) Position of flowering time QTL detected for each environment (in black), for plasticity parameters (slope_Tmean, ICPA1, IPCA2, IPCA4, IPCA6, ICPA7 in purple), and for the overall mean flowering time across the nine environments (in green) obtained using the multi-environment model (MEM). Significant QEI in the MEM are written in red. Linkage groups (LG) are ordered by male and female linkage maps. Red lines, Bayesian credible intervals common to the different QTL detected in 3A_M, 6A_M and 6D_M QTL.

(B) Venn diagram of QTL detected for flowering time and plasticity parameters. Mean: QTL detected by environment for the mean flowering times or with the MEM for the overall flowering time; Plasticity parameters: QTL detected for slope_Tmean (slopeTm), ICPA1, IPCA2, IPCA4, IPCA6, ICPA7; QEI: QTL-by-Environment Interactions detected with the MEM. QTL detected for the overall mean with MEM are in bold.

(C) LOD scores of QTL and QEI obtained for the multi-environment model: in green the LOD curve for main and interactive effects, in red the LOD curve for the interactive term alone. Thresholds, $\alpha = 5\%$.

(D) Variation in QTL effects for flowering time. Only QTL detected by environment are represented ($\alpha = 5\%$).

QTL are named according to the LG where they were detected. M and F, male and female linkage maps respectively. SP, Spain, IT, Italy, FR, France, GE, Germany, PL, Poland. 2018 and 2019 (18 and 19 respectively), years of experimentations.

Figure 5. Allelic effects of flowering time QTL.

(A) Effect of the 6D_M QTL on flowering time according to mean temperature calculated from the 1st of January until end of flowering. QTL effects: significant (black point) or non-significant (grey point).

(B) Effect of alleles of the three major QTL (respectively 6D_M, 3A_M, 6A_M) on flowering time (GDD). Significant pairwise differences levels between allelic classes at the three markers are indicated by stars following a Kruskal-Wallis test (ns, non-significant).

(C) Allele Specific PCR (KASP) assay developed on the 6D. The green and purple dots represent the homozygous genotypes (C/C and T/T) and the orange dot represents heterozygous genotypes. The gray dots represent the non-template control.

(D) Effect of the KASP_6D marker on flowering time in the 'Candonga' x 'Senga Sengana' segregating population (left) and in a set of 94 genotypes (right).

(D) Allelic effect of the KASP_6D marker on flowering time in the 'Candonga' x 'Senga Sengana' segregating population (left) and in a set of 94 genotypes (right).

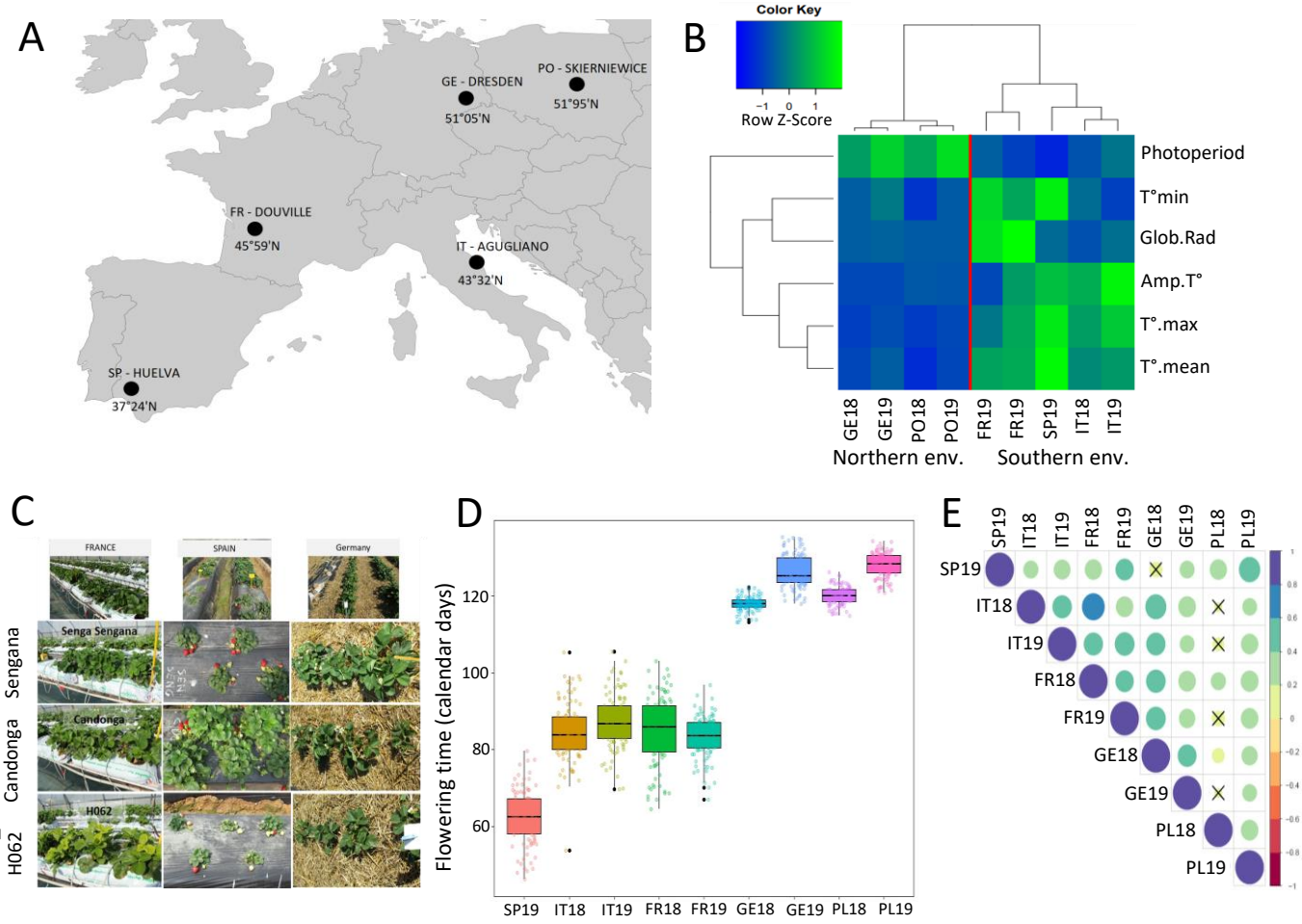

Figure 1. Environment description and flowering time of the 'Candonga' x 'Senga Sengana' segregating population in nine environments.

(A) Location and latitudes of the five countries in which experimental trials were carried out.

(B) Clustering of the nine experimental environments according to the six environmental covariates measured from the 1st of January until end of flowering.

(C) Three genotypes, 'Candonga', 'Senga Sengana' and 'H062' under three environments in 2018 (France, Spain and Germany).

(D) Box plots showing the flowering time (calendar days) for the nine environments.

(E) Pairwise Spearman correlation values (r) between flowering time (calendar days) in the nine environments. The r values are represented by coloured circles whose size varies according to their value. Crossed-out circles indicate non-significant correlations (*p*-value > 0.05).

SP, Spain, IT, Italy, FR, France, GE, Germany, PL, Poland. 2018 and 2019 (18 and 19 respectively), years of experimentations. Sites are ordered by increasing order of latitude.

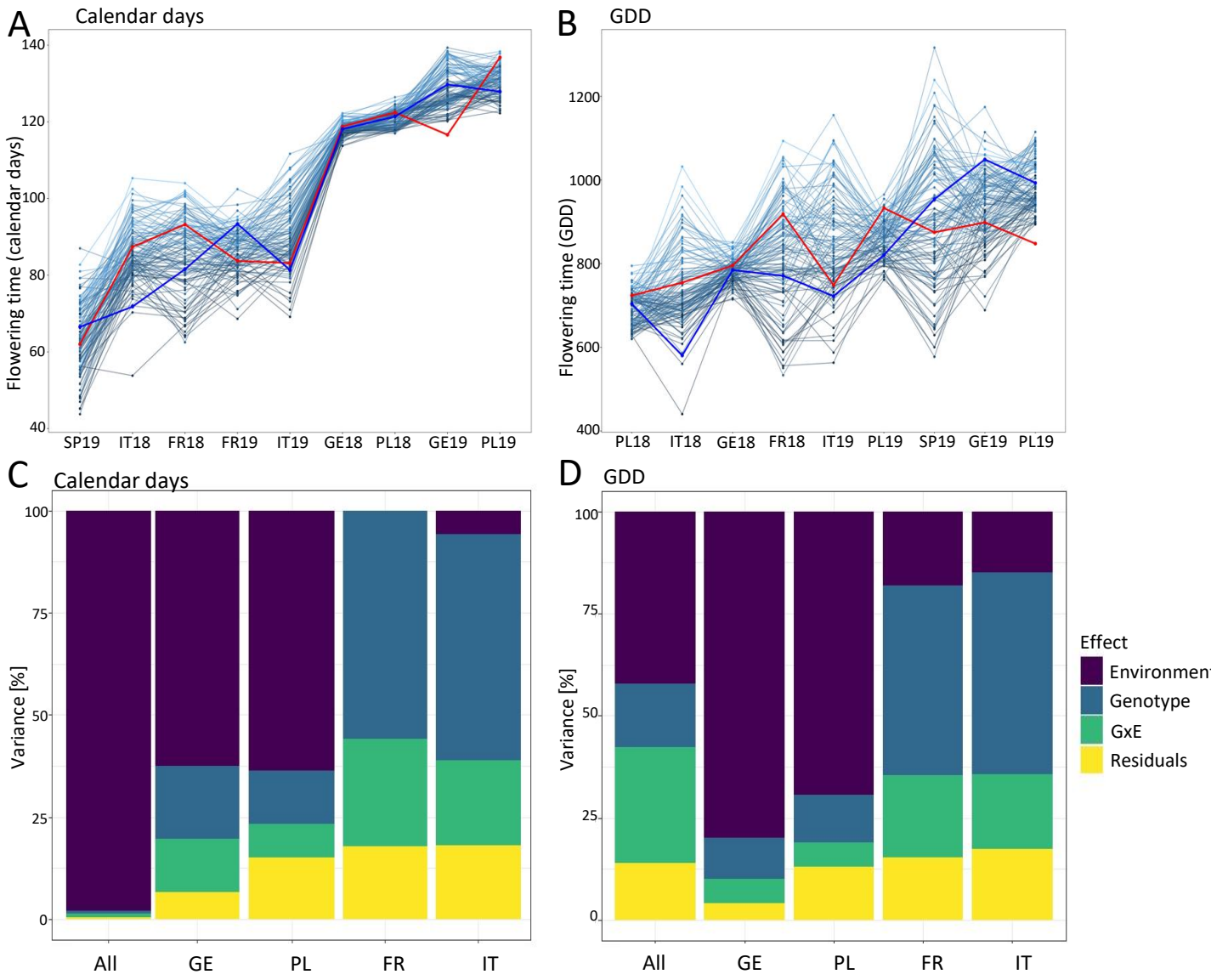

Figure 2. Reaction norms and analyses of variance for flowering time.
(A-B) Reaction norm for flowering time expressed in calendar days (A) or Growing Degree-Days (GDD) (B). The nine environments are ranked in increasing order of flowering time. Each line connects the flowering time values of individuals across environments. Red and blue lines represent 'Candonga' and 'Senga Sengana' respectively.
(C-D) Variance partitioning of flowering time (calendar days (C) and GDD (D)) by the linear mixed model for the nine environments or for each country.
SP, Spain, IT, Italy, FR, France, GE, Germany, PL, Poland. 2018 and 2019 (18 and 19 respectively), years of experimentations.

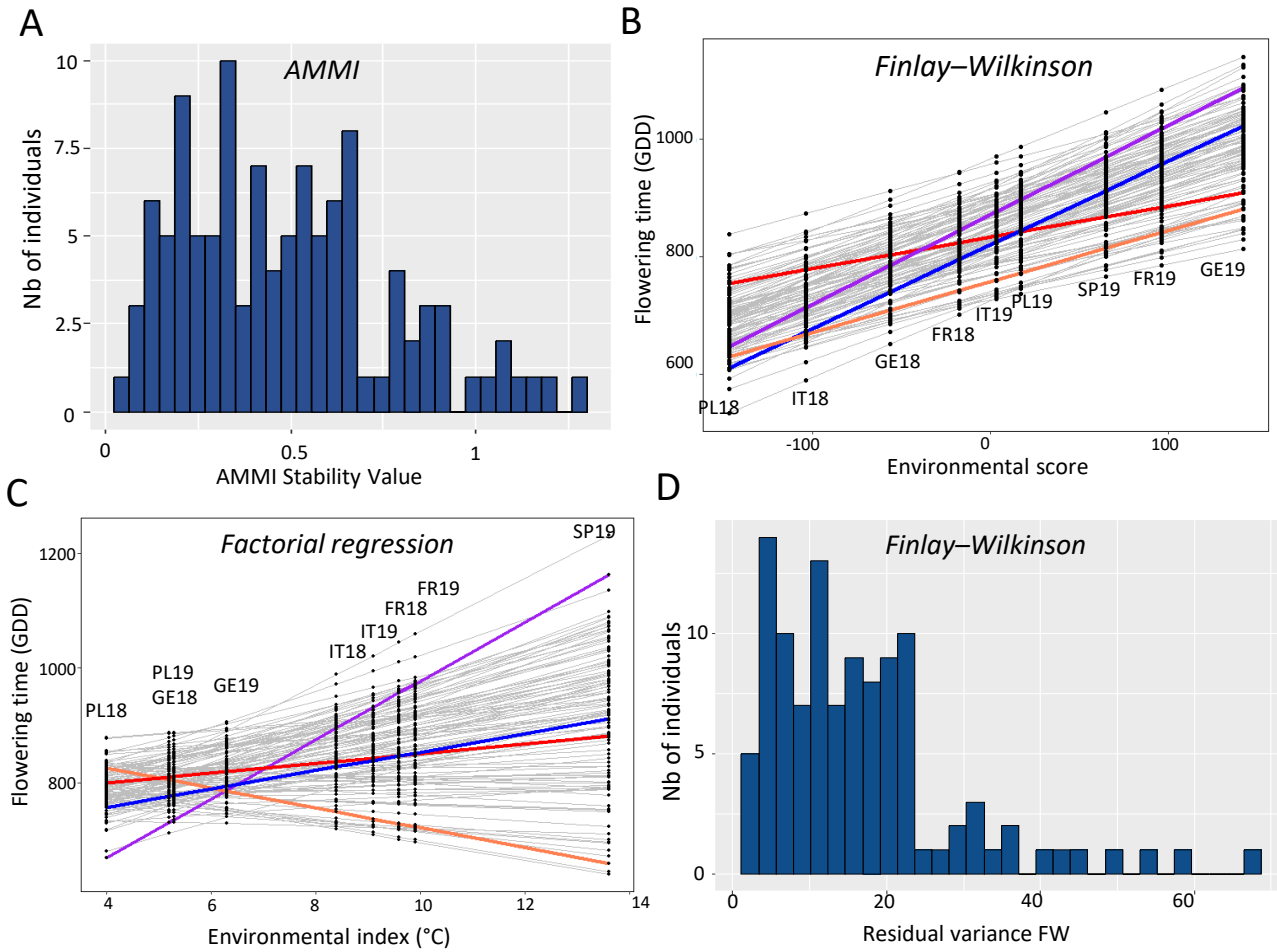

Figure 3. Distributions of plasticity parameters for all individuals and parents in the segregating population for flowering time.

(A) Histogram distribution of AMMI Stability Values (ASV) calculated for each genotype as the relative influence of IPCA1 and IPCA2 scores based on the sum of squares of their interaction.

(B-C) Slopes with Finlay–Wilkinson and factorial regression models for flowering time (GDD). Regressions of phenotypic performances of genotypes on environmental index (B) or on mean temperature (C). 'Candonga', 'Senga Sengana', 'H102' (example of a late flowering genotype) and 'H056' (example of an early flowering genotype) are plotted as red, blue, purple and orange lines, respectively.

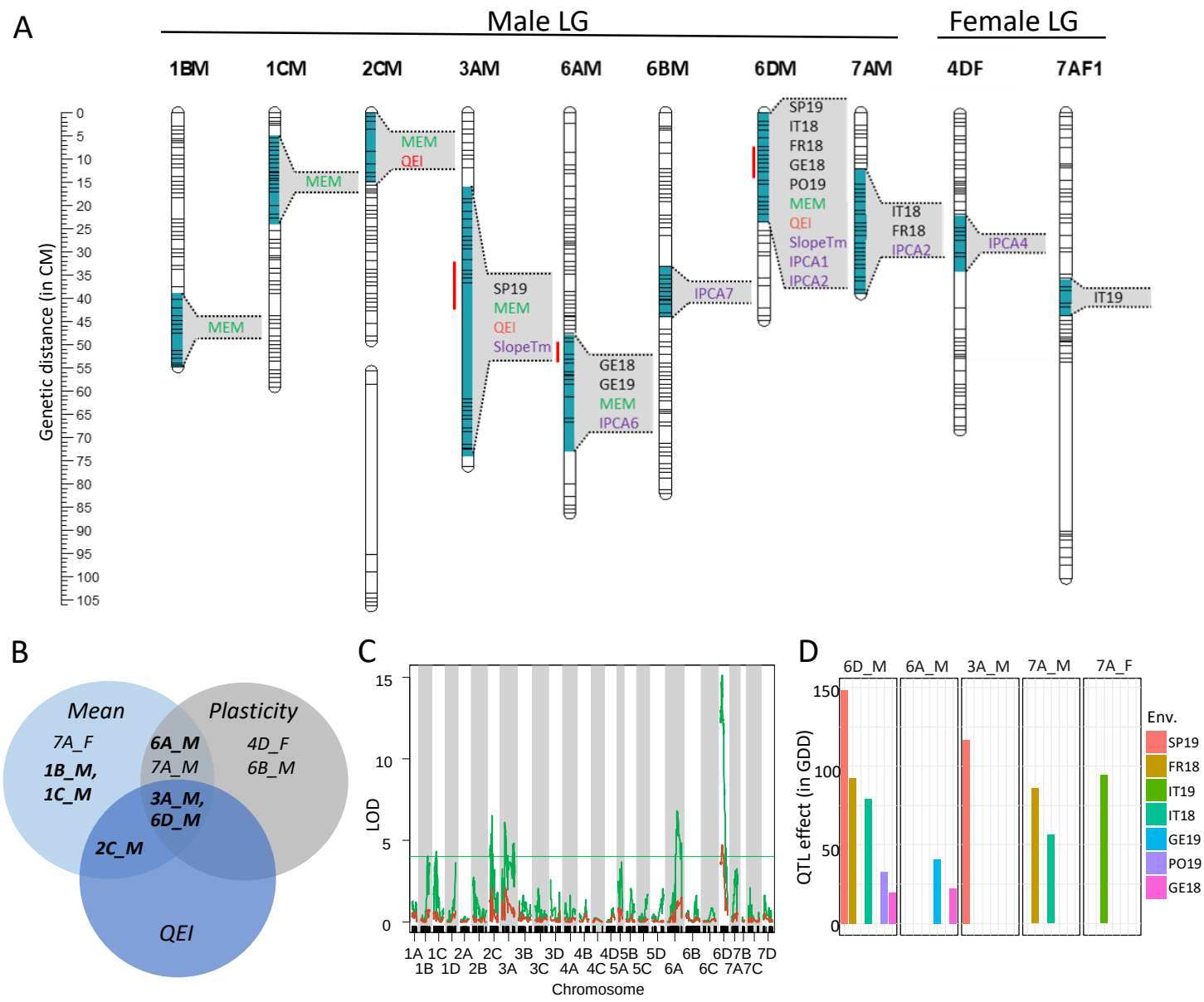

Figure 4. Effects of flowering time QTL and QTL-by-Environment Interactions (QEI).

(A) Position of flowering time QTL detected for each environment (in black), for plasticity parameters (slope_Tmean, ICPA1, IPCA2, IPCA4, IPCA6, ICPA7 in purple), and for the overall mean flowering time across the nine environments (in green) obtained using the multi-environment model (MEM). Significant QEI in the MEM are written in red. Linkage groups (LG) are ordered by male and female linkage maps. Red lines, Bayesian credible intervals common to the different QTL detected in 3A_M, 6A_M and 6D_M QTL.

(B) Venn diagram of QTL detected for flowering time and plasticity parameters. Mean: QTL detected by environment for the mean flowering times or with the MEM for the overall flowering time; Plasticity parameters: QTL detected for slope_Tmean (slopeTm), ICPA1, IPCA2, IPCA4, IPCA6, ICPA7; QEI: QTL-by-Environment Interactions detected with the MEM. QTL detected for the overall mean with MEM are in bold.

(C) LOD scores of QTL and QEI obtained for the multi-environment model: in green the LOD curve for main and interactive effects, in red the LOD curve for the interactive term alone. Thresholds, α = 5%.

(D) Variation in QTL effects for flowering time. Only QTL detected by environment are represented (α = 5%).

QTL are named according to the LG where they were detected. M and F, male and female linkage maps respectively. SP, Spain, IT, Italy, FR, France, GE, Germany, PL, Poland. 2018 and 2019 (18 and 19 respectively), years of experimentations.

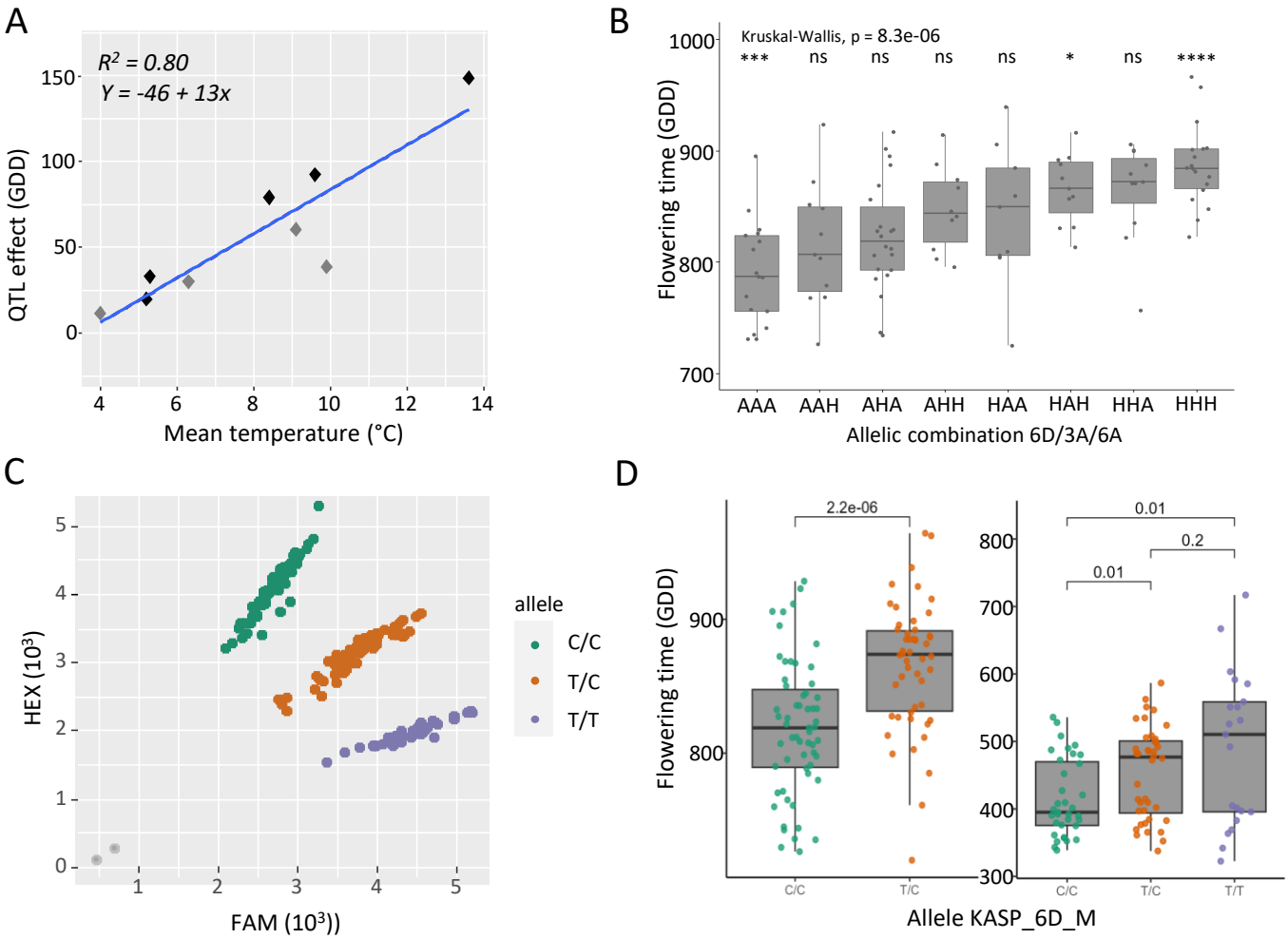

Figure 5. Allelic effects of flowering time QTL.
(A) Effect of the 6D_M QTL on flowering time according to mean temperature calculated from the 1st of January until end of flowering. QTL effects: significant (black point) or non-significant (grey point).
(B) Effect of alleles of the three major QTL (respectively 6D_M, 3A_M, 6A_M) on flowering time (GDD). Significant pairwise differences levels between allelic classes at the three markers are indicated by stars following a Kruskal-Wallis test (ns, non-significant).
(C) Allele Specific PCR (KASP) assay developed on the 6D. The green and purple dots represent the homozygous genotypes (C/C and T/T) and the orange dot represents heterozygous genotypes. The gray dots represent the non-template control.
(D) Effect of the KASP_6D marker on flowering time in the 'Candonga' x 'Senga Sengana' segregating population (left) and in a set of 94 genotypes (right).